Chapter 1: Science Goals and Requirements

1.1. Understanding Small-scale Elementary Magnetic Structures

1.1.1. Elementary Structures Connecting from Photosphere to Corona

The Hinode mission provides both the first high-resolution diagnostics of the solar magnetic field and from a space platform, and is now allowing scientists to discover the processes by which the magnetic flux interacts with the solar convective flows in the lower solar atmosphere (the "photosphere"). One of major improvements on our knowledge is that horizontal oriented magnetic fields are ubiquitously distributed over the solar surface (Lites et al. 2007) and that they are dynamically evolved on the photosphere (Centeno et al. 2007, Ishikawa et al. 2007). Furthermore, Hinode has provided strong indications that the convective motions initiate outward propagating waves and dynamic reconnection events that result in heating of the plasma accompanied by significant outward mass flux (e.g., Isobe et al. 2008). One of new features revealed with Hinode observations is that many of chromospheric "Type-II" spicules show substantial transverse displacements during their short lifetimes (<100s), which is interpreted as propagation of Alfven waves along magnetic field in the chromosphere (De Pontieu et al. 2007). This observation also suggests that energy transport takes place via magnetic structures whose width is **~0.3 arcsec at the chromosphere**. Moreover, another important observational feature is that the spectral lines emitted from the corona at temperatures of 2MK show excess non-thermal line broadening at the footpoints of coronal loops, caused by weak component that is highly blue-shifted to in order of 100 km/s (Hara et al. 2008). Existence of highly blue-shifted features may suggest that numerous number of small transient energy releases, i.e., nanoflares, take place at the base of coronal loops (More details will be discussed in section 1.2).

For understanding the heating of corona and acceleration of the solar wind, it is now the most essential to quantitatively and exactly identify how the energy (such as mass flow, magnetohydrodynamic waves with fast mode, slow mode, and Alfven mode, and localized heating by nanoflares, and flux emergence) is transported to the corona through the chromosphere and transition region, which have a complex system of magnetic fields with full variety of plasma dynamics. Observations are required to distinguish the two competing theories for coronal heating, i.e., mechanical heating by upward-propagating waves, and Joule heating associated with magnetic reconnections. Quantitative identification is needed for different magnetic structures, such as active region, quiet Sun and coronal holes, because the manifestation of the energy transport is varied depending on the natures of magnetic field structures.

To distinguish transport mechanisms, it is very important challenge to resolve the dynamical nature of small-scale elementary magnetic structures in the complicated photosphere-chromosphere-corona system. Furthermore, dynamical nature and evolution of elementary structures formed in upper atmosphere is directly connected to the formation of global magnetic field structures and the magnetic energy storage and release that causes the violent dynamical events (flares and CMEs).

1.1.2. Elementary Structures of Coronal Magnetic Loops

Although the EUV images obtained by TRACE and SDO/AIA (spatial resolution about 0.5arcsec) showed thin coronal loops (Figure 1.1), it is not clear that elemental structures in corona are resolved. Aschwanden & Nightingale (2005) investigated the thermal structure of coronal loops based on the TRACE multi-filter analysis, and found that the width of the isothermal loops is 1000~2000 km. If we define the width of an elemental loop by the homogeneous temperature cross-section, we can say that TRACE resolved the elemental structure in corona. On the other hand, the EUV spectroscopic measurements with EIS on Hinode show that the volumetric filling factor of coronal loops is approximately 10% (Warren et al. 2008); With the spatial resolution of 2-3arcsec (pixel size 1arcsec), only 10% of the volume in coronal loops are filled with hot plasma. It means that a coronal loop is constructed from fine threads with the width in order of ~200 km (0.3arcsec) or less. Thus, there is the disagreement between the filling-factor analysis based on EUV spectra and the temperature analysis based on the EUV line images. Doschek et al. (2010) showed that small coronal bright points, particularly prominent in coronal holes, has internal structure in the corona, although their morphological structure are not spatially resolved with the current available instrument (Figure 1.2). Hence, to understand the elementary structures in corona, we need to resolve not only the stable structures but also the dynamic structures with high time resolution.

Figure 1.1. A magnetically active region at the edge of the Sun shows "loops" that connect one magnetic polarity to the other. A coronal image (Fe IX in 171A) from TRACE. Coronal structures seen with 0.5 arcsec spatial resolution.

The EUV spectrometer with the spatial resolution of ~0.3 arcsec, which is about one order of magnitude higher than EIS resolution, (and the normal incidence X-ray telescope with the spatial resolution of 0.2 arcsec as the second option), will be able to almost resolve coronal loops at fundamental scales. That is, spatial scales at which loops behave coherently and can be described by simple hydrodynamic models. The combination of the filling-factor analysis with the EUV spectrometer and coronal images at 0.1 arcsec pixel from the X-ray imaging telescope makes clear what the elementary structure of coronal loops is. For this purpose, the X-ray telescope with normal incidence optics may be more suitable than the photon-counting telescope.

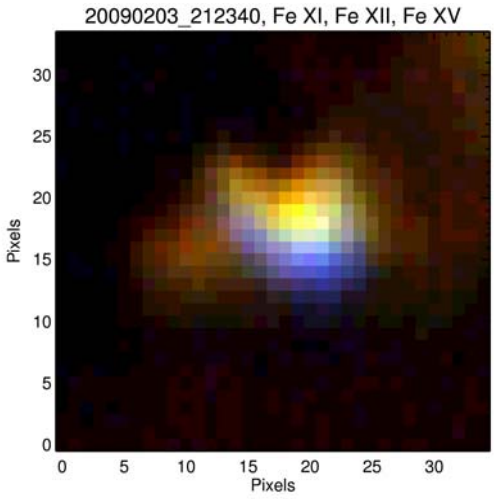

Figure 1.2. A polar coronal hole bright point in lines of Fe XI (red), Fe XII (green), and Fe XV (blue). The bright point looks like an unresolved flare seen by Yohkoh.

1.1.3. Elementary Structures in Dynamical Chromosphere

The chromosphere is the region that interfaces the gas-pressure-dominated photosphere and the magnetic-field-pressure-dominated corona, through which ionization fraction and the plasma beta change drastically. The chrompsphere forms the conduit for the upward flux of mass and energy, while most of the non-radiative energy is dissipated there to supply the heat. Hinode observations demonstrate that the chromosphere is extremely dynamic: small scale structures called as straws, jets, or fibrils cover the entire surface of the Sun, high speed chromospheric 'jets' (type-II spicules, de Pontieu etal 2007) have a width of ~0.3arcsec and change with a time scale of 10 second or less. It is obvious that the chromosphere cannot be considered as an atmospheric 'layer', but it is a wholly dynamic 3D entity that never settles to hydrostatic equilibrium. Even in the most quiet area of the Sun, i.e., in the very quiet photospheric "internetwork", the chromosphere appears to be dominated by largely acoustic shocks, which are initiated in the photosphere by the solar convection and the global p-mode oscillations. Strong "network" fields exist in the photosphere at the boundaries of the internetwork. These fields spread rapidly with height in the highly stratified chromosphere, and at some height they form a magnetic canopy over the internetwork regions. Recent observations from Hinode and other instruments have suggested that the network fields, interacting with convection, energize and structure the quiet chromosphere. Dynamic phenomena in the chromosphere are more dominating in active regions, where apparent reconnection events occur frequently, producing outward propagating jets that may be seen at coronal temperatures (e.g., Shibata et al. 2007, Figure 1.3).

High-speed jets in quiet Sun (type-II spicules) are, however, only visible near the solar limb with Hinode imaging observations, because of their insufficient optical thickness on the disk under the Hinode's Ca II H band-pass filter. In addition, Hinode provides only morphological information of such chromospheric features. With the lack of the Doppler information, the nature of the type-II spicules in quiet regions or those in sunspot penumbrae (Katsukawa et al. 2007) are still under debate. One of important question is whether they are real plasma ejections with the apparent speed along the magnetic fields or not. Without answering the question, we cannot know their physical origin. To understand the generation mechanism and consequence of this fundamental ingredient of the chromospheres, we definitely need velocity

information with better contrast and higher spatial and temporal resolutions. The proposed Solar Ultra-Violet Visible and IR telescope (SUVIT) has a large aperture (1.5 m diameter is now under study), which can achieve a spatial resolution better than 0.06arcsec in Mg II 280nm line. This UV line provides unprecedented images of fine-scale chromospheric structures with much higher contrast. The supreme spatial resolution allows us to explore plasma motions and magnetic-field behaviors inside the chromospheric structures with ~0.3arcsec width. Observations of full spectral line profiles allow us to study the real plasma flow along the magnetic fields with its acceleration and density distribution, and also to clearly identify the connectivity to their photospheric (or possibly chromospheric) root points. The high sensitivity, high-resolution Doppler images (Dopplergram) of chromospheres will for the first time detect the elementary plasma motions, which would be associated with wave shocks and magnetic reconnections, and thus provide a concrete basis of energetic in the chromosphere.

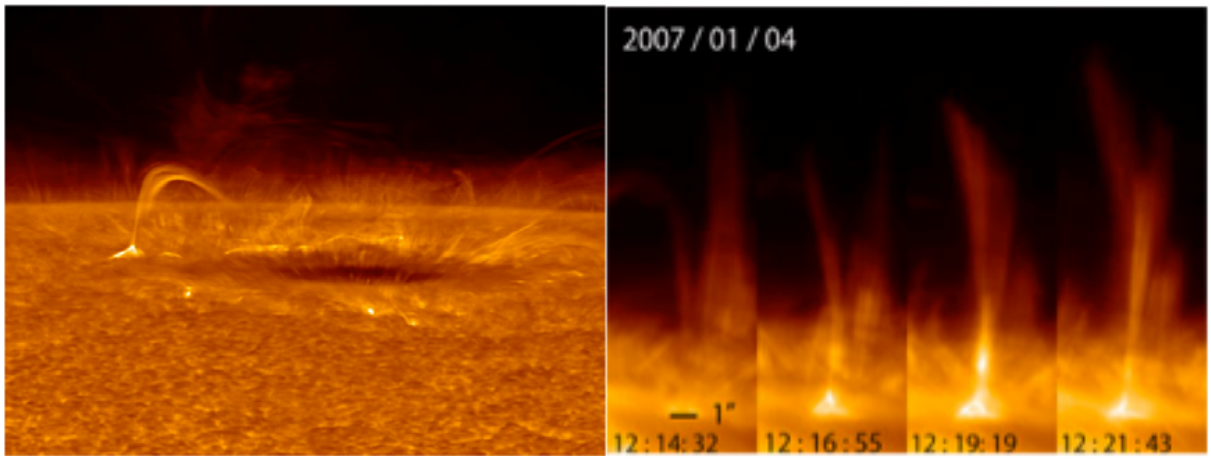

Figure 1.3. Dynamical chromosphere observed with Hinode. (Left) Dynamical chromospheric features around a large sunspot (Right) Chromospheric jets.

Ubiquitous chromospheric jets associated with cusp-shaped structures (Figure 1.3) show a hint of intermittency of plasma ejection, which infers the presence of more elementary reconnection processes. SUVIT aims to identify any non-stationary motions or intensity fluctuation in and around the reconnection site to understand the basic physics that controls the rate of fast reconnection taking place in the chromospheres (See also Section 1.3). One particular interest regarding the magnetic reconnection is the injection of magnetic helicity into the magnetic fields during the reconnection of obliquely directed two flux tubes. Spectroscopic information in a higher spatial resolution will detect the twist or twisting motions in a flux tube, which may be crucial importance for dynamics of the ejected plasma or even for global evolution of the corona. Moreover, SUVIT provides the direct measurements of the magnetic fields in particular chromospheric features like the reconnection cusp. Even with less spatial and temporal resolution in polarimetric observations, such direct information of magnetic fields at the reconnection site is of a fundamental importance to establish the reconnection models of the chromospheric dynamics. Enigmatic phenomena, such as the Ellerman bombs around sunspots (Matsumoto et al. 2008) and intermittent and recurrent occurrence of chromospheric plasma ejections from sunspot light bridges (Shimizu et al. 2009), are also important targets with a great interest relating to the magnetic field reconnection.

1.1.4. Elementary Structures in Photosphere

Photosphere is the region where the gas pressure dominates the magnetic force and, as a result, the kinetic energy of plasma is transferred into the energy of magnetic fields. The magnetic fields are discretely distributed and highly localized into tiny magnetic flux tubes. Hinode SOT aimed to resolve the magnetic flux tubes that have a size of 0.2 - 0.3 arcsec (Figure 1.4, e.g., Nagata et al. 2008), and revealed that they are continuously shaken by surrounding convective eddies, interacting with each other (merge and split), and occasionally newly formed and canceled out. These motions of magnetic elements in the photosphere are the plausible source of the generation of waves propagating upward and magnetic activities such as ubiquitous reconnections taking place in the upper atmosphere. Individual magnetic elements are detected, however, with only one or a few pixels in SOT magnetograph (Figure 1.4), and it is impossible to infer their internal structures. Thus we are still missing the information of electric currents and shape of the cross section of the flux tubes, which are of a crucial importance for understanding the real energetics of fine scale magnetic fields of the Sun. Furthermore SOT frequently observes anomalous Stokes profiles that infer the presence of unresolved magnetic structures and supersonic flows in photosphere (e.g., Shimizu et al. 2008).

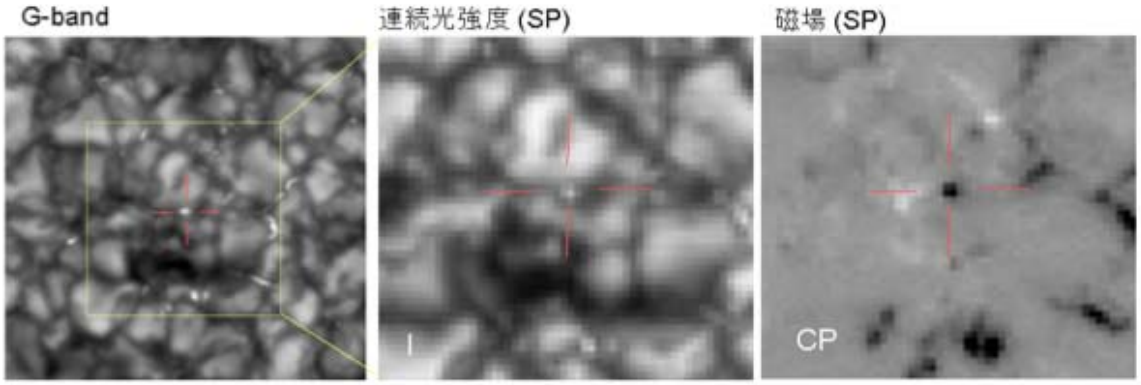

Figure 1.4. A magnetic flux tube captured with Hinode SOT.

The proposed 1.5 m telescope (SUVIT) will observe the interaction between the elementary magnetic structures and the convection in the photosphere to scrutinize the process of energy injection into the magnetic fields in much grater detail; with a 0.1arcsec spatial resolution (pixel scale dx < 0.05") and with the same photometric accuracy with SOT/Hinode (Figure 1.5), SUVIT achieves a sensitivity to the magnetic field (dBlong x $(dx)^2$) and the associated energy elements (j^2 = (dBtang x $dx)^2$) one order of magnitude higher than SOT (Figure 1.6). SUVIT will detect the twist, i.e., the electric current, of individual flux tubes and their evolutions. Temporal variation of electric current is an important signal of a small-scale energy dissipation in upper atmosphere. Interaction of flux tubes with vortices in granular convection is of particular interest for understanding the generation of electric currents and torsional waves in flux tubes. The distribution of magnetic field and velocity across the flux tube and its time variation will provide a clue to identify the mode of waves propagating along the flux tubes. Resolving possible 'hidden' magnetic polarities in a 'uni-polar' region with a higher spatial resolution is very important to understand the mechanism of ubiquitous chromospheric jets taking place over there. The most notable advantage of SUVIT is that it can continuously observe a system of magnetic flux elements in a wide field of view with a highest possible resolution, accuracy and large time coverage under a seeing-free condition. Such observation

enable us to track the evolution of foot points of the magnetic field system and, for the first time, provides a chance to capture a small scale manifestation that triggers the eruption of a magnetic system.

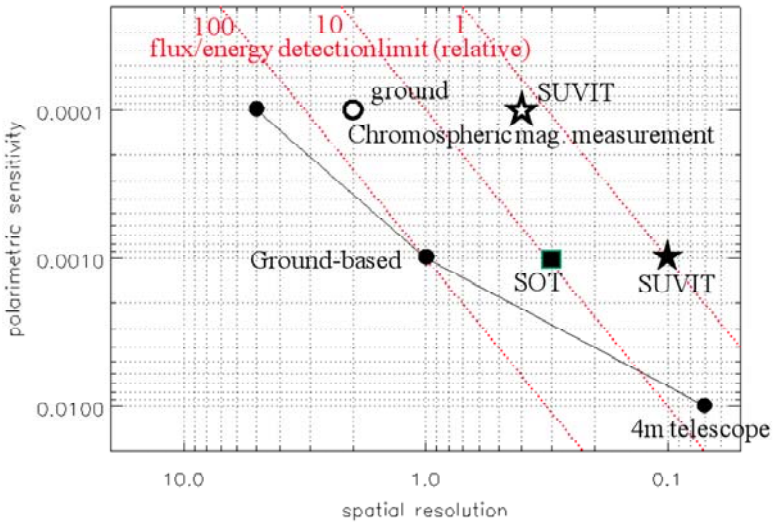

Figure 1.5. Solar-C, Hinode, and ground-based observations on the plane of the spatial resolution vs. photometric sensitivity. High S/N observations for chromospheric magnetic field are shown by open symbols. Detection limits for magnetic flux and energy element are shown by oblique dashed lines.

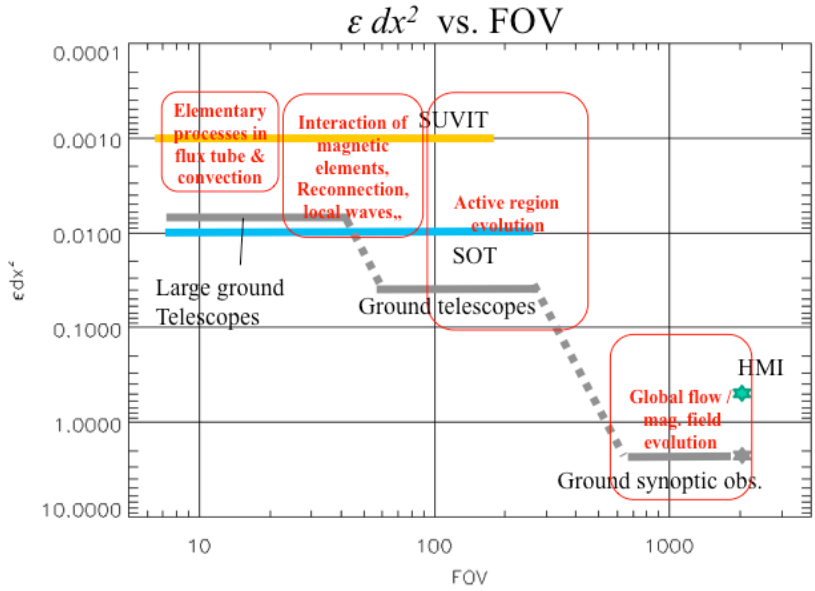

Figure 1.6. The sensitivity to the magnetic flux and energy elements (εdx^2) and the field of view (FOV) of SUVIT and other observations. The SUVIT sensitivity is compared with Hinode SOT and ground-based observations. The unit in the vertical axis is arbitrary and the horizontal axis in arcsec. The figure also shows the sensitivity range and FOV of the observations required for 4 specific science topics.

A similar argument can be applied to the Doppler measurements too; i.e., SUVIT has a 10 times higher sensitivity than SOT to the kinetic energy of gas motions. Tiny flows and shocks possibly associated with photospheric magnetic reconnections, but not resolved so far, are one

of the important targets of SUVIT observations. Observing the dynamic interactions of the magnetic fields with ubiquitous shocks generated by granular convection in the photosphere may provide a direct clue on the origin of spicules or transient phenomena in chromosphere.

These fundamental plasma processes postulated to be taking place in the high β photospheric plasma are only accessible with high accuracy spectro-polarimetric measurement at 0.1" resolution under a very stable imaging condition, which can be only realized from the space.

1.2. Understanding Energy Transport through Small-scale Structures

As briefly described in section 1.1, two non-thermal mechanisms have been debated to explain the heating of corona and acceleration of the solar wind: upward-propagating waves along the magnetic structures, and Joule heating associated with magnetic reconnections. Further observations are required to distinguish how the two mechanisms are excited in the dynamical atmosphere at the elementary structure scale, how the non-thermal energy can be transported with the mechanisms toward the chromosphere, transition region and corona, and how the transported energy can be used to heat the atmosphere and accelerating the plasma. Particularly, the energy transport through small-scale magnetic structures should be observationally understood to distinguish the roles of the two mechanisms in the heating.

1.2.1. Connecting the Chromosphere to the Corona

Hinode imaging observations revealed that substantial transverse displacements exist in many of chromospheric "Type-II" spicules (De Pontieu et al. 2007). Moreover, with coordination with measurements of EUV spectral lines oriented from the transition region (TR), a blue-red asymmetry was derived in TR spectral lines, suggesting that "Type-II" spicules transport mass towards the corona (De Pontieu et al. 2009, McIntosh & De Pontieu 2009). Furthermore, the spectral lines oriented from the corona at temperatures of 2MK show excess non-thermal line broadening at the footpoints of coronal loops, which can be seen only when the coronal loops are observed from the top (i.e., disk center view) (Hara et al. 2008). Based on these Hinode observations (Figure 1.7), quantitatively evaluating of mass and energy transport between the chromosphere, TR, and the corona at the base of coronal loops is essential to reach the conclusion for the coronal heating puzzle.

TR (transition region) is the interface connecting between 20,000 K (upper chromosphere) and 1 MK (corona). SOHO, Hinode and previous space missions have shown the TR to be a highly dynamic and structured region. SUMER high-resolution spectro-heliograms reveal that, on the quiet Sun, the lower-mid TR ($T < 700{,}000$ K) is formed by many loop-like structures 10″ to 20″ long located along and across network boundaries. Similar but fainter structures are also seen in cell centers. From these data it seems that the majority of the TR emission, particularly on the quiet Sun, may not represent a continuous transition between the chromosphere and the corona. EIS raster scans also show the transition from the small-scale TR structures to large-scale coronal loops and funnels to occur around 0.7 to 0.8 MK (Matsuzaki et al. 2007).

Of course, transition region "interface" regions must exist at the footpoints of loops or funnels reaching coronal temperatures but they appear to be responsible for only a small fraction of the TR emission. This would naturally explain the fact that the TR emits much more than it would do if it were a very thin (few tens of km) thermal layer, heated by thermal conduction from the hot corona (as in classical, static, 1-D models). On the other side, SOHO

observations have also shown the TR to be very dynamic on time scales of the order of 10 s to 100 s.

Quiet Sun TR loops also do not seem to have obvious magnetic counterparts at photospheric levels, indicating that the loop footpoints are connected to multiple magnetic elements in the photosphere via a complex system of field lines (Sanchez-Almeida et al. 2007). A similar phenomenon is also observed in moss areas, regions of enhanced EUV emission in upper TR and low coronal lines at the footpoints of 3 MK to 5 MK coronal loops in active regions. In this case their emission is mainly due to thermal conduction from the hot loops. Each footpoint of coronal loops is rooted into a uni-polar magnetic plage region, where no mixed polarity magnetic flux elements are observed at the photospheric level, suggesting a complex magnetic coupling in the upper atmosphere (Brooks et al. 2009).

Therefore, measuring magnetic fields in the higher atmosphere, i.e., chromosphere, would be crucially important for unveiling the nature of this complex coupling between loop-like structures in TR and the photosphere. At the same time, the EUV spectrometer probes all temperature ranges from the upper chromosphere up to the corona with high spatial, spectral, and temporal resolution. The TR strongly emits in the UV/EUV (160 to 2,000 Å) and lines from increasingly higher ionization stages generally fall at shorter wavelengths. The EUV spectrometer should cover a very wide spectral range at unprecedented spatial and temporal resolution, allowing, for the first time, the full characterization of this region of the solar atmosphere: from the topology and morphology of the magnetic structures to the thermodynamic state of the plasma (its motions, density, temperature and abundances) that fills these structures.

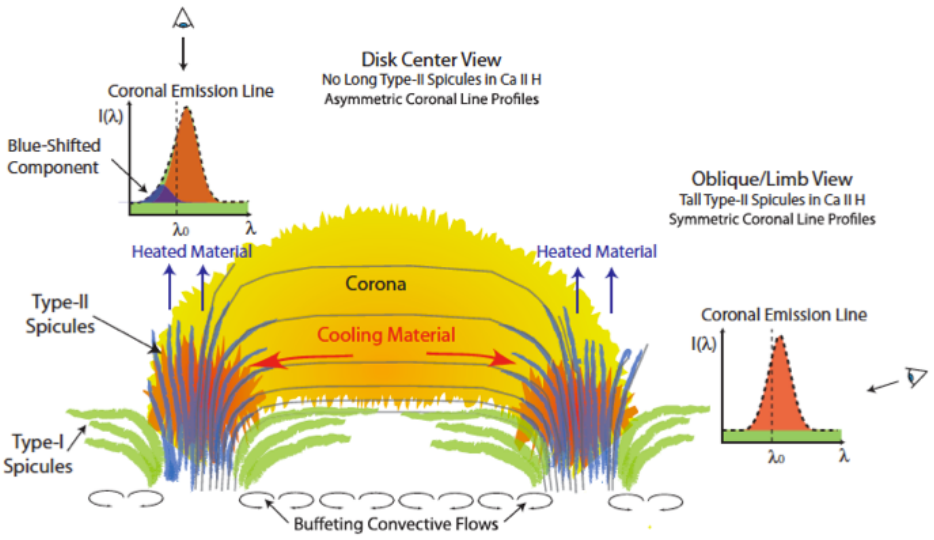

Figure 5. Mass and energy transport between the chromosphere, TR, and corona, as deduced from SOT and EIS observations. See Section 4 for details.

Figure 1.7. Schematic illustration of mass and energy transport between the chromosphere, TR, and corona for the closed loop systems (from De Pontieu et al. 2009)

1.2.2. Magnetohydrodynamic (MHD) Waves in the Solar Atmosphere

Recent observations, especially Hinode's imaging observations, have clearly revealed the presence of apparent transverse oscillations, which are affirmative evidence of the Alfven waves, in the chromosphere and corona. Wave-like oscillations are observed in a wide variety

of solar structures, such as prominence in the corona (Okamoto et al. 2007, Figure 1.8), spicules (de Pontieu et al. 2007, Figure 1.9), and Ca II H dynamical jet (Nishizuka et al. 2008) with Hinode SOT.

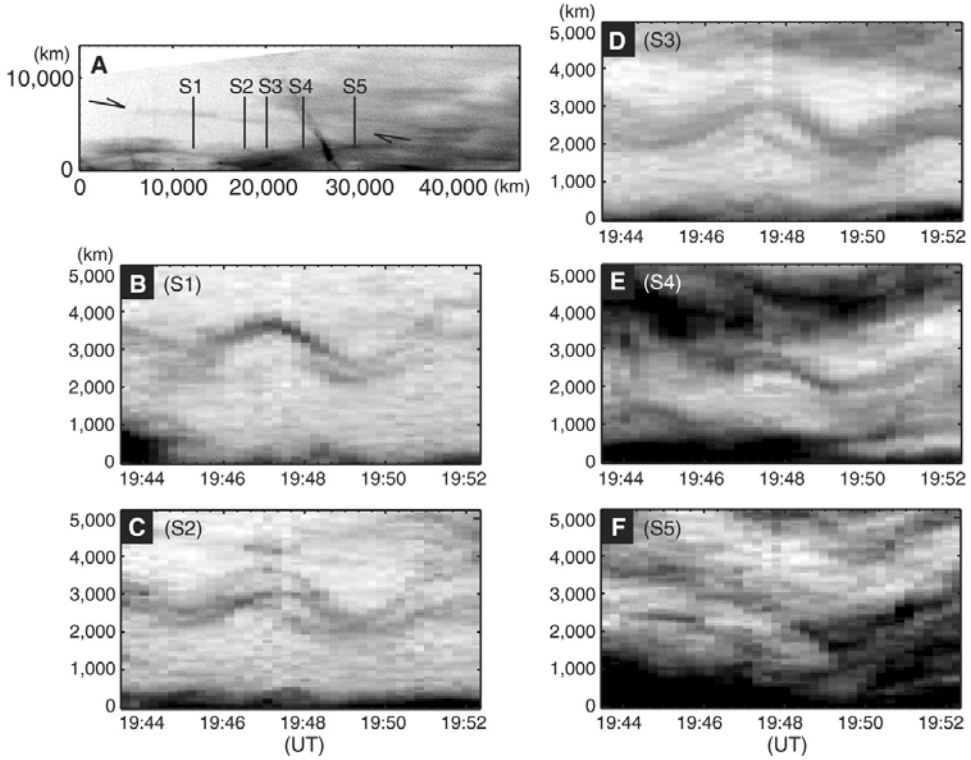

Figure 1.8. Example of a prominence thread undergoing synchronous oscillation along its entire length (from Okamoto et al. 2007)

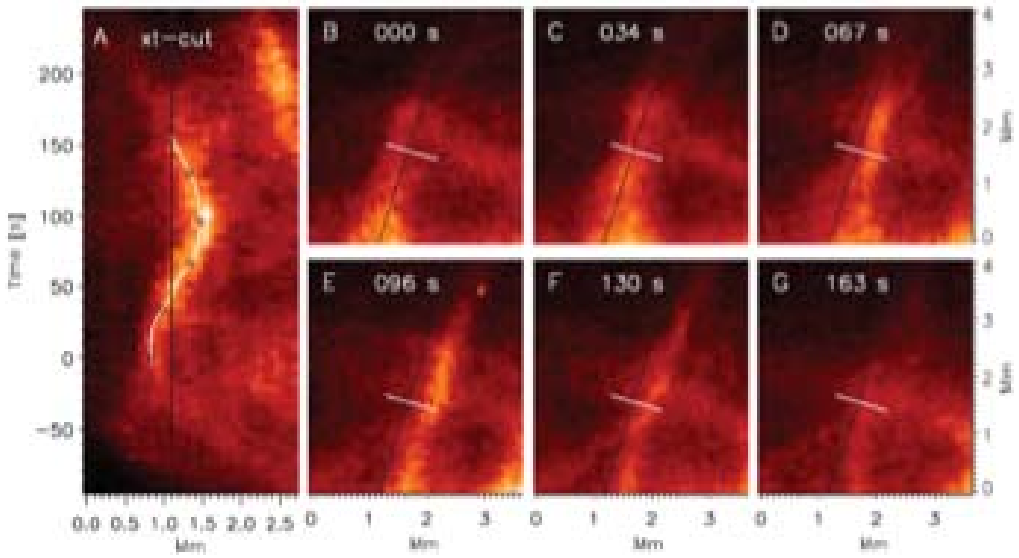

Figure 1.9. Example of the transverse displacement of a spicule (from de Pontieu et al. 2007)

However, we did not identify whether the observed waves are really propagating Alfven waves, or just standing waves in most of observations, except for ubiquitous upward waves in the corona detected with a coronagraph measurement of line-of-sight velocity fluctuations (Tomczyk et al. 2007). Thus, in order to evaluate the propagating MHD waves and their modes, observations require not only velocity and photometric measurements (Kitagawa et al 2010)

but also the measurements of the magnetic field fluctuation, as examined with photospheric magnetic-field data by Fujimura and Tsuneta (2009).

1.2.2.1. Relevance of Observed Waves for Chromospheric Energy Budget

The chromosphere's temperature is approximately 10,000 K with high density. To maintain the temperature structure of the chromosphere, it is required to input heat in the chromosphere about one order of magnitude higher than that required for heating the corona.

Recent studies show that there is insufficient acoustic wave power propagating at higher-frequencies (>5mHz) from the solar interior to heat the chromosphere (Fossum & Carlsson 2005; Carlsson et al. 2007). However, it is shown that inclined magnetic field lines at the boundaries of large-scale convective cells provide portals through which low-frequency (<5mHz) magnetoacoustic waves can propagate in the chromosphere (Suematsu 1990), and these waves provide a significant source of the energy necessary for balancing the radiative losses of the ambient chromosphere (Jefferies et al. 2006). When magnetoacoustic waves propagate upward in strongly stratified atmosphere such as the chromosphere, the waves will steep into shocks to heat the chromosphere (Carlsson & Stein 1997). Carlsson, Hansteen & Gudiksen (2010) indicates that as low-frequency magneto-acoustic shock waves interact with small magnetic elements, joule heating may be effective at these elements' edges.

It is important to observationally determine how much energy is sustained in observed waves, with identifying the mode of the waves. The energy should be measured as a function of magnetic field inclination and atmospheric height. To determine the power of magnetoacoustic waves at the lower atmosphere, we need the measurements in cadences of better than 10-20 seconds with line-of-sight velocity amplitudes of ~0.1 km/s for the photospheric lines and with ~1 km/s for chromospheric lines (e.g., Vecchio et al. 2007). High spatial resolution, 0.1-0.2 arcsec, is needed to resolve individual channels for wave propagation (Bogdan et al. 2003). Moreover, determining the importance of shocks is vital for balancing the radiative losses in the more magnetized parts of the upper chromosphere. To do this, velocity measurements with UV lines in formation temperatures between 10^4 and 10^5 K need to be coordinated with the photospheric and chromospheric measurements with visible lines. For measurements with UV lines, we need cadences of better than 20-30 seconds, which provide 6-15 measurements in one period of 3-5 minutes oscillations, and Doppler velocity measurements of better than 10 km/s (equivalent to sound speed in the upper chromosphere) with line width measurements of better than 5 km/s. It is also important to have the capability to resolve the elemental structures where the wave power is channeled. These are typically on the order of 0.3-0.4" in size, inferred from the observed width of spicules. The wide temperature coverage will allow us to track the evolution of the wave power as it propagates through the different layers of the solar atmosphere. We should note that the NASA IRIS mission, which will be launched in late 2012, will provide new information on the chromosphere, especially on the line-of-sight velocity amplitude measured with chromospheric lines, but it does not have adequate transition region and coronal coverage, nor will it measure chromospheric magnetic fields, both of them are essential to evaluate the natures of magnetoacoustic waves in the solar atmosphere.

1.2.2.2. Time Series Spectra at Different Atmospheric Layers

The problems encountered in understanding the coupling between the chromosphere and the corona are illustrated in Figure 2.2-4. The chromosphere has relatively large patches (10″ to 20″) of many thin, bright spicules (width~0.3"), and the coronal structures are narrow, isolated loops that fade at their footpoints. There is little correspondence between the two. A

comparable transition region image that can only be obtained by a rastering spectrometer would take almost two hours to complete with the current available spectrometer such as SUMER. Although the large-scale structures do not normally change on this timescale, the small-scale dynamics are much faster, and thus high-cadence spectroscopic measurements in transition region lines will make a giant step forward. Moreover, matching spatial resolutions both below (chromosphere and photosphere) and above (transition region and corona) is crucially important to trace the energy flow over the entire atmosphere.

As illustrated in Figure 1.10, spectral lines show different characteristics among chromosphere (Cauzzi et al. 2007), transition region, and corona. The chromospheric spectra have characteristic 3 to 5 min periods, the transition region brightenings occur in bursts of up to 30 min (Innes et al. 1997), while coronal variations are more diffuse. Such different characteristics would reflect the energy transport and release at each layer, but no one knows details, because this kind of time series spectra has never been recorded simultaneously with different spectral lines covering the solar atmosphere with 0.3" spatial resolution.

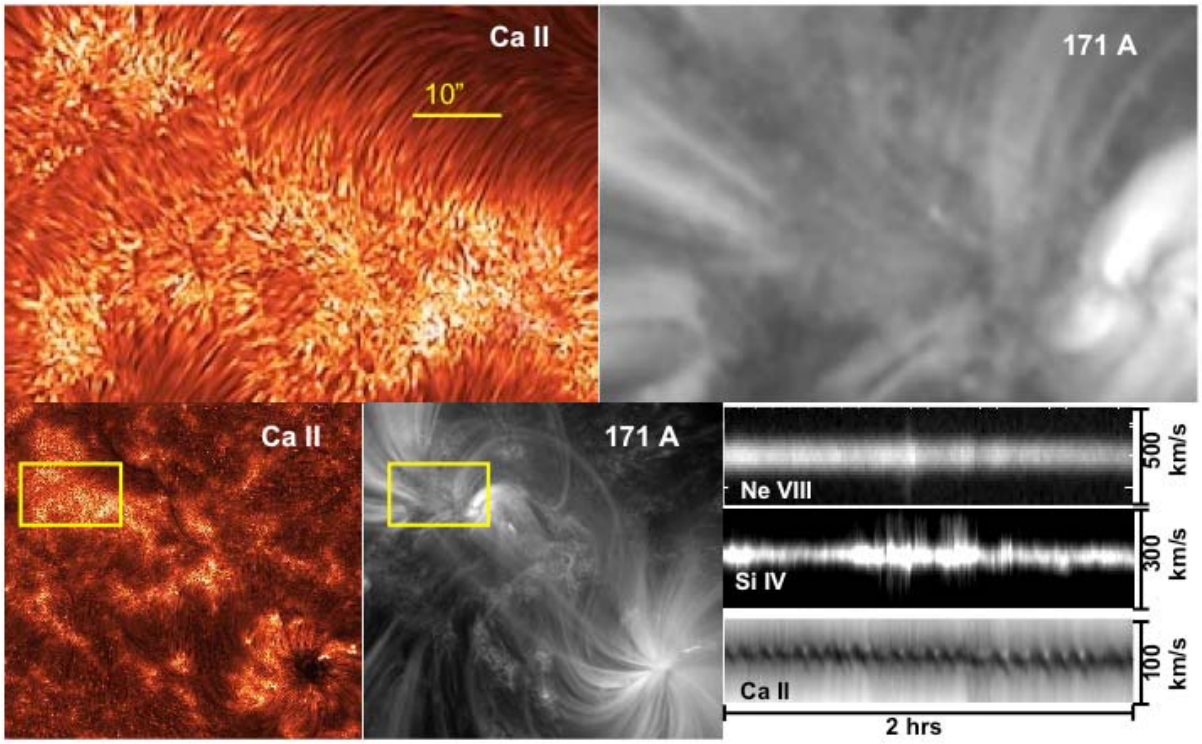

Figure 1.10. The chromosphere-corona connection. The top panels show cut-outs taken from the chromosphere (Ca II, with spatial resolution ~ 0.3") and the lower corona (171A, with spatial resolution ~1″) images. The regions are outlined in yellow. The bottom right panel shows representative time series of chromospheric (Ca II), transition region (Si IV), and lower coronal (Ne VIII) line profiles (recorded at different regions at different times).

The diffuse spectra in coronal lines is much wider than thermal line broadening due to high temperature plasma, and the extra broadening has been considered as non-thermal line broadening. The origin of the non-thermal broadening is uncertain, but it may reflect turbulent nature in the coronal loops. Hinode observations have revealed that the non-thermal line broadening is well observed at the footpoints of coronal loops and that the non-thermal broadening is more enhanced when the coronal loops are viewed from the top, suggesting that there are high-speed upflows which are not resolved spatially (Hara et al. 2008). With having

shorter exposure with ~0.3" spatial resolution, the non-thermal broadening may be partially resolved as Doppler shift signatures of jets in each elementary magnetic structure.

1.2.2.3. Alfven Waves' Contribution to Heating Corona and Accelerating Solar Winds

Alfven waves, transverse magnetohydrodynamic waves that can propagate along the magnetic field lines over large distances and transport magneto-convective energy from the photosphere into the corona, are one promising candidate for the energy source both for the acceleration of the solar wind and for the heating of the quiet corona.

Numerical simulations have been made these days to investigate the nonlinear propagation of Alfven waves in the highly stratified atmosphere. Alfven waves are significantly attenuated in the stratified atmosphere between the photosphere and transition region by various dissipation processes such as nonlinear mode conversion, Alfven wave resonance and phase mixing. Suzuki and Inutsuka (2005) showed that the limited portion of the waves is able to propagate to the corona and nonlinear low-frequency Alfven waves can simultaneously heat the corona and drive the fast solar wind. By using the temporal spectrum of the convection motions at the photosphere from Hinode observations, Matsumoto and Shibata (2010) showed that the observed convection motions generate Alfven waves and that the region between the photosphere and the transition region becomes an Alfven resonant cavity.

The currently available observations of oscillation events do not allow us to determine whether sufficient energy would remain in the waves that penetrate all the way to the corona to make a substantial contribution to the heating budget of the solar corona and/or the acceleration of the solar wind. For allowing this evaluation, observations are required to clearly identify propagating Alfven waves and their modes in the region between the photosphere and the transition region. Such observations are the measurements of the magnetic field fluctuation at the chromosphere and the simultaneous measurements of velocity and photometric information from the chromosphere to the transition region.

1.2.2.4. Specific Topics to be Addressed by New Observations

In addition to evaluating how much energy is sustained in observed waves over the atmosphere, the following questions can be newly addressed with these unique observations. All of them cannot be studied at all with currently available instruments. First, mode conversion of waves may occur around the layer where the plasma beta becomes unity (e.g., Bogdan et al. 2003). Since the beta~1 layer is around or below the middle chromosphere, we may detect the signature of mode conversion in waves. The phase relation between velocity and magnetic field fluctuations will tell how observed waves behave in stratified atmosphere, depending on magnetic structures. Secondly, high throughput performance of the proposed EUV/FUV spectroscopic telescope can allow a search for higher frequency waves and a search for wave signatures in line widths and velocity in the transition region and corona. For active region observations, the telescope will have 1-5 sec exposure time for intense spectral lines with 0.3 arcsec spatial sampling, and 0.5-1 sec exposure time for about 1 arcsec spatial sampling. Slit-and-stare measurements will provide the temporal series of spectral lines with higher cadence than 1 sec, allowing a search for higher frequency waves and thus obtaining new insights in heating of the active region corona by high frequency waves. Thirdly, we may obtain fine-scale structure of magnetic fields by measurements of vector magnetic fields at the chromosphere. We can directly study the properties of turbulent cascade or phase mixing of Alfvenic waves by these small scale magnetic structure. For instance small-scale current sheets

in the chromosphere would be an evidence for phase mixing. Anisotropic elongated structure along magnetic fields would be an evidence of cascade of Alfvenic turbulence.

1.2.3. Signatures of Energy Dissipations in the Corona

An outstanding issue that remains elusive in the formation and evolution of coronal loops is the localization of energy conversion. As an alternative to the classic nanoflare model with magnetic reconnection at coronal heights (Parker et al. 1989), it has been recently suggested that reconnection takes place in the chromosphere and is responsible for the coronal heating through the formation of jets and spicules (e.g., Aschwanden, Nightingale & Alexander 2000). As mentioned previously, recent Hinode observations indicate high-speed upward mass flows at small scale and excess non-thermal line broadening at the base of coronal loops, suggesting that the origin of coronal heating exists in the base of the coronal structures (section 1.2.1).

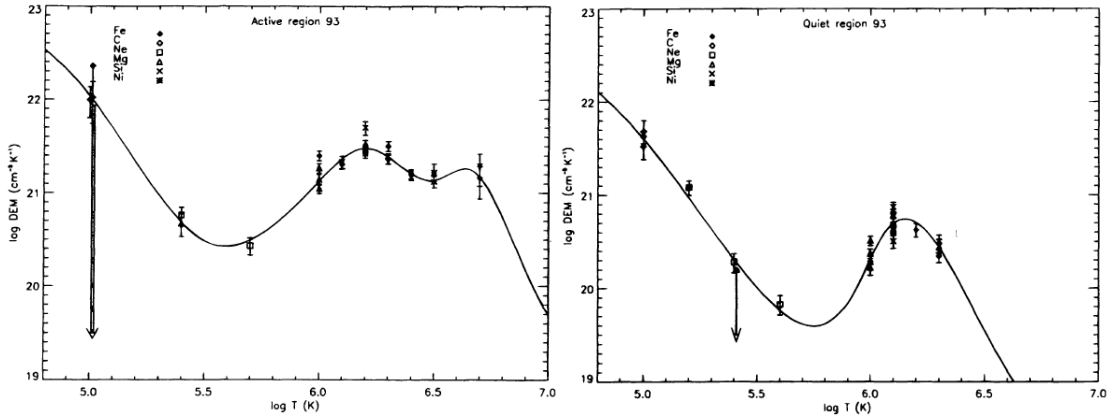

Figure 1.11. *Left:* Differential emission measure (DEM) distribution for an active region. Note no emission line is available for temperature diagnostic beyond logT = 6.7 (T = 5 MK). *Right:* DEM distribution for quiet Sun. After Brosius *et al.* 1996.

High temporal and spatial resolutions are needed to resolve the evolution of numerous, small-scale explosive events like a nanoflare "storm" (Klimchuk, 2006). This tells us whether continuous heating changing slowly compared to a cooling time or impulsive heating repeating rapidly compared to a cooling time is more significant for the coronal heating process. In addition, plasma diagnostics capabilities in the broad temperature coverage, such as measurements of the differential emission measure (DEM, Figure 1.11), electron density, or turbulent velocities, are crucial to advancing the understanding of coronal heating. Also, the pair of EUV emission lines from different atomic species allows us to estimate the thermal temperature of ions because of the difference in their thermal velocities (Imada et al. 2009). The EUV spectrometer proposed for Solar-C is the ideal instrument for the plasma diagnostic because of its sub-arcsec spatial resolution, EIS-like or better spectral resolution, wide temperature coverage from the photosphere into the corona, and high throughput. The EUV spectrometer has the diagnostic capabilities for the plasma only up to ~5 MK, because high-temperature plasma in 3-6MK is energetically dominant in active-region corona (Figure 1.11). There is also an interesting indication from Hinode XRT that there possibly exist high-temperature components whose temperature at least 5 MK (could be as high as 10 MK) diffusely distributing across the quiet Sun, even without any active regions (Ishibashi et al. 2011). High-temperature components can be created by energy dissipations in the corona.

Identification of temperatures of such components in the corona, coupled with their spatial distribution, may provide important clues on how the corona is heated, and maintains its temperature. If the proposed photon-counting X-ray telescope is selected as the X-ray imaging telescope, it will reveal high-temperature temperature components and their temporal evolution by obtaining spatially-resolved X-ray count spectra.

1.2.4. Behaviors of Magnetic Fields in Corona Explored through Seismology

It has been difficult to measure magnetic field fluctuation in the corona, which is one of key information to investigate propagating waves. However, observations of oscillations in the corona have the potential to reveal different properties of the local plasma environment. For example, kink-mode transverse oscillations of the coronal loops impulsively excited by the blast wave in a large flare (Nakariakov et al. 1999, Figure 1.12) can be recognized in the time series of coronal images and allow us to estimate the value of the local magnetic field strength. In some cases, both fundamental mode and higher harmonics are obtained, which enables us to estimate the density stratification along coronal loops.

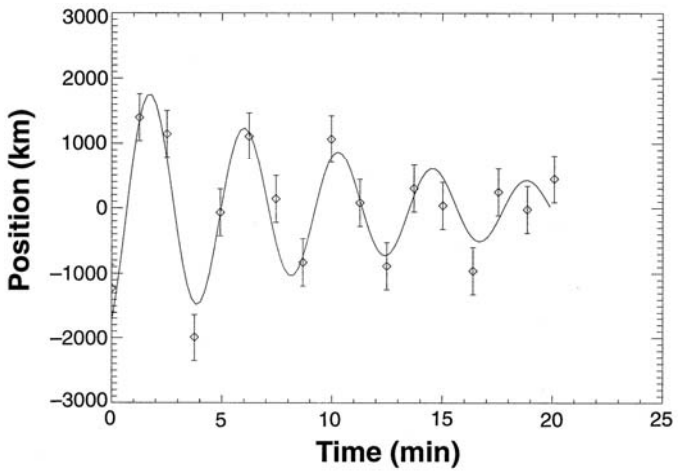

Figure 1.12. Temporal evolution of the loop displacement through the loop apex when oscillation is exited in the loop (Nakariakov et al. 1999)

The Solar-C observations will allow us to take Doppler velocity measurements of such oscillating loops. Oscillations of coronal loops during Alfven waves propagate along the loops may be measured with the proposed EUV spectrometer, which may derive local magnetic field strength as a function of the distance from the base of coronal loops. The techniques of coronal seismology require cadences of the order of 2 s (Roberts 2000) to determine radially dependent parameters. By having higher spatial resolution (~0.3”), the density and temperature can be measured in the configuration that different coronal loops are less overlapped. This allows to have better estimate on the density and the local field strength. Direct measurement of velocity is a key parameter, because linear Alfvén waves are incompressible and so do not show up as intensity perturbations. The velocity resolution needed to observe the perturbations caused by these waves is of order 10 km s^{-1} to see spatially resolved waves and 5 km s^{-1} should be these waves on smaller scales than we can resolve.

1.3. Magnetic Reconnection

1.3.1. The Solar Atmosphere as a Laboratory for Magnetic Reconnection

Magnetic reconnection is one of the most important mechanisms for the plasma heating and particle acceleration in magnetized space and astrophysical plasmas. The importance of magnetic reconnection is well discussed in many plasma environment, such as the Earth's magnetosphere (e.g., Hones, 1979; Nagai et al., 1998, 2001; Baumjohann et al., 1999; Øieroset et al., 2002; Imada et al., 2005, 2007, 2008), laboratory (e.g., Baum & Bratenahl, 1974; Ono et al., 1997; Ji et al., 1998; Yamada et al., 1997), and also the solar atmosphere. Several astronomical phenomena, such as accretion disks, proto-type stars, AGN jets, cluster of galaxies, and pulser wind, are also recently simulated and discussed with magnetic reconnection to explain dynamical natures revealed with X-ray and radio observations.

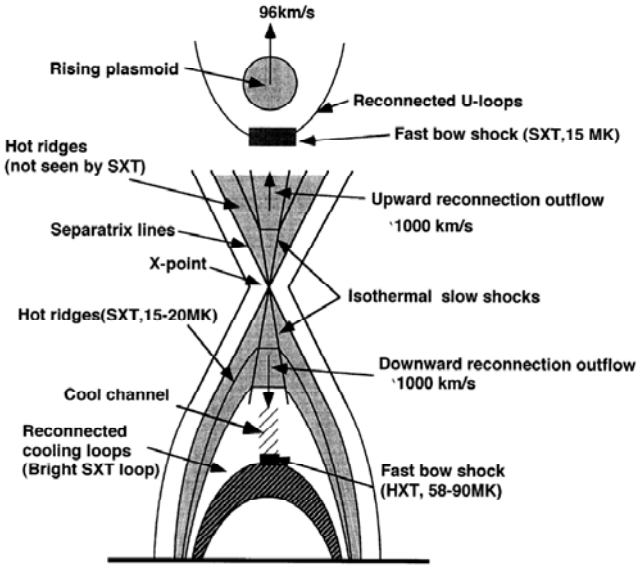

Figure 1.13. Global magnetic configuration and associated reconnection signatures in a type of solar flares (Tsuneta et al. 1997).

Magnetic reconnection is believed to be central to the energy release in solar flares, the heating of the solar corona, and the initiation of coronal mass ejections (CMEs) (Figure 1.13). It is a rapid mechanism for converting the stored magnetic energy into kinetic, thermal, non-thermal and wave/turbulence energy via magnetic dissipation process. Yohkoh X-ray observations provided some pieces of evidence for magnetic reconnection in solar flares and coronal jets, and then Hinode has revealed that magnetic reconnection occurs with various configurations of magnetic fields not only in the corona but also in the chromosphere. The energy conversion by magnetic reconnection is fundamental and essential to explain dynamical behaviors in the wide variety of plasmas in the solar atmosphere. While considerable progress has been made over the past decade, three key questions listed below have not yet been answered with observations:

1) What plasma conditions and parameters, such as collisionality or temperature, control the energy release rate of magnetic reconnection (reconnection rate)?
   → Section 1.3.2 and 1.3.3
2) What determines the energy distribution among kinetic, thermal, wave/turbulence, and especially non-thermal energy at the rapid conversion of stored magnetic energy? → Section 1.3.4 and 1.3.5
3) What is the role of 3-dimensionality in magnetic reconnection? → Section 1.3.6

Observations carried out by the Solar-C Plan B mission should be designed to answer these questions.

1.3.2. Magnetic reconnection occurring in a wide variety of plasma conditions

One of the fundamental questions in magnetic reconnection is what determines the energy release rate. It is also what fraction of released energy is converted into kinetic, thermal, non-thermal, and wave/turbulence energies. Previous studies of solar, space and laboratory plasmas challenged these questions, though they have not yet answered these questions. The solar atmosphere shows us a wide variety of plasma conditions, i.e. weakly ionized to fully ionized plasmas, and collisional to collisionless plasmas (Table 1.1), which are quite different from the plasma conditions in magnetosphere or laboratory experiments. Observational investigation of magnetic reconnection under various plasma conditions is very important for space, solar, astrophysical and laboratory plasma physics. The challenge of the Solar-C mission is to diagnose magnetic reconnection in such various plasma conditions with more direct observational information available from spectroscopic measurements in three different wavelengths (IR-visible-UV, FUV-EUV, and soft X-ray). Especially, the proposed high throughput UV/EUV spectroscopic telescope can reveal plasma dynamics in faint reconnection region with high cadence measurements, and the proposed photon-counting X-ray telescope will enable us to diagnose particle acceleration mechanism with imaging spectroscopy in X-rays. The spectro-polarimetric instrument of the proposed IR-visible-UV telescope measures the magnetic fields in the chromosphere, allowing us to understand chromospheric reconnection more detail.

Table 1.1. Typical properties of plasma in solar atmosphere

	Photosphere	Chromosphere	Inner Corona	Outer Corona (~2Rs)
Dominant pressure	Gas	Magnetic field	Magnetic field	Gas
Ionization	Neutral	Weakly ionized	Fully ionized	Fully ionized
Collisionality	Collisional	Collisional	Semi-collisionless	Collisionless

1.3.3. Magnetic reconnection in weakly ionized plasma (solar chromosphere)

1.3.3.1. Does fast reconnection really occurs in the chromospheres?

One of the most important Hinode findings is that magnetic reconnection events frequently occur in the solar chromosphere. Shibata et al. (2007) found the ubiquitous presence of chromospheric anemone jets outside sunspots in active regions. The anemone jets have an inverted Y-shape, similar to the shape of X-ray anemone jets in the corona (Figure 1.3). Their typical velocity is comparable to the local Alfven speed in the lower chromospheres, and their footpoints are located among the mixed polarity region. So they concluded that chromospheric anemone jets imply magnetic reconnection in the chromospheres.

Hinode has also discovered new types of magnetic reconnection events in the chromospheres with various magnetic field configurations (e.g. Katsukawa et al. 2007, Nishizuka et al. 2008, Shimizu et al. 2009). Shimizu et al. (2009) revealed that sunspot light bridges sometimes show recurrent occurrence of chromospheric jets. Vector magnetic field data in the photosphere suggests that a helical magnetic flux tube lying below the light bridge plays vital roles in producing jets. Katsukawa et al. (2007) also found microjets even in the sunspot penumbra, where magnetic field lines are usually not fully anti-parallel.

One of the important questions about magnetic reconnection in the solar chromosphere is whether the magnetic reconnection in the chromosphere is really fast, independent on resistivity, or not. Our current guess, which is based on Hinode observations, is ”yes”. Hinode Ca II H movies, however, do not allow us to evaluate the reconnection rate. The time cadence of the Ca II H observations is fast enough, but quantitative information, such as plasma flows, density, temperature and magnetic field, are needed. These quantitative parameters are available from the proposed IR-visible-UV telescope

1.3.3.2. Observations of Ambipolar effect in weakly ionized plasma

Chromosphere is high density, collisional and weakly ionized plasma. In such a condition, it is hard to expect fast reconnection. On the basis of the space and laboratory plasma observations, it is said that, to drive “fast reconnection”, “anomalous resistivity” should work in the diffusion region via microscopic process. To make it possible, the following two aspects should be satisfied: ion gyro radius is larger than mean free path (collisionless condition), and the width of a current sheet becomes thin comparable to ion gyro radius. However, it seems that Sweet-Parker current sheet is not so thin, and the mean free path in the lower chromosphere is smaller than ion gyro radius. If fast reconnection really occurs in the chromosphere, additional physics should be considered.

One candidate is “ambipolar effect” in the chromosphere, where the neutral hydrogen to proton density ratio is $\sim 10^4$ (i.e. Singh and Krishan 2010). Ambipolar diffusivity is effective in the chromosphere because of the ion-neutral collisions. The collision between ions and neutrals causes ambipolar diffusion, which plays a role in making a current sheet thinner and thinner in the weakly ionized plasma (e.g., Zweibel, 1988, 1989, Brandenburg & Zweibel, 1994, Chiueh, 1998). Isobe et al. (in preparation) discussed the effect of ambipolar diffusivity and showed that bursty reconnection can take place in the chromosphere (Fig 1.14). The nature of magnetic reconnection in the chromosphere is still not clear from both observational and theoretical viewpoints. The aim of the Solar-C mission with the IR-visible-UV spectro-polarimetric

observations is to measure physical parameters around the reconnection region and observationally determine the reconnection rate qualitatively and to reveal the dynamics of magnetized plasma in various configurations of magnetic field with direct observation of chromospheric vector magnetic field.

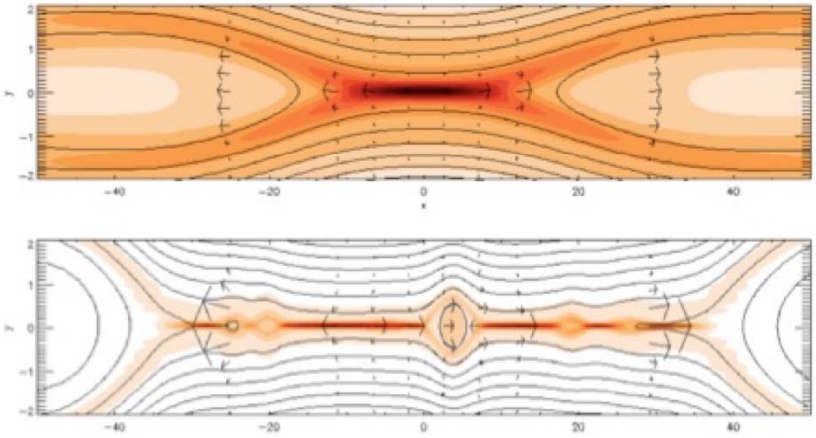

Figure 1.14. Magnetic reconnection in weakly ionized plasma (bottom) and collisionless plasma (top).

1.3.4. Magnetic reconnection in collisonless plasma (corona and transition region)

Magnetic reconnection in the solar corona has been discussed as a key mechanism involved in solar flares. Various features expected from the magnetic-reconnection model have been confirmed with modern space observations. For example, Yohkoh observed the cusp-like structure, which is predicted by the standard reconnection flare model (Tsuneta et al., 1997). Quantitative understanding in the key region of solar flares, however, is not enough so far to discuss the energy release rate or energy distribution rate of magnetic reconnection.

The primary reason why it is difficult to directly observe the magnetic reconnection region is because of its faintness. A bright cusp-like structure (flare loop) is formed during a solar flare, and the reconnection region that is believed to exist above the cusp structure is extremely faint. A large dynamic range of intensity and low-scattering performance is required to observe inside the reconnection region. Moreover, since the temperature in the reconnection region may be significantly higher than that of cusp-like flare loops (e.g., Tsuneta et al., 1997), the line spectral signature (ionization state) in the reconnection region may be different from what seen in flare loops.

1.3.4.1. What determines the energy distribution among kinetic, thermal, wave/turbulence, and non-thermal energies?

One of the important parameters for magnetic reconnection in the solar corona is how much energy is stored in the coronal magnetic fields. The stored energy can be estimated from the magnetic-field measurements at the photosphere (Top part of Fig 1.15). For example, Kubo et al. (2007) showed magnetic-field evolution of a flare productive active region with continuous series of photospheric magnetic fields by Hinode. Magara and Tsuneta (2008) calculated the magnetic helicity in the flare-productive active region and found that the helicity increases very rapidly before the flare. This quantitative analysis is very important for the estimation of stored energy before magnetic reconnection. Reconnection electric fields (reconnection rate) also can

be quantitatively estimated with Hinode (e.g. Jing et al., 2008). Therefore, we can observationally evaluate the stored magnetic field energy and its release rate, which is the top part of Fig 1.15.

To understand the energy distribution among the energies, we need to evaluate each of thermal, kinetic, non-thermal, and wave/turbulence energies during a flare. Spectroscopic observations with EIS on board Hinode enable us to evaluate thermal energy with differential emission measure analysis (e.g., Watanabe et al. 2007), kinetic energy with the Doppler velocity analysis (e.g., Asai et al., 2008), wave/turbulence energy with line broadening analysis (Imada et al. 2008), and non-thermal energy with simultaneous RHESSI hard X-ray and microwave observations (e.g. Minoshima et al. 2009, Watanabe et al. 2010).

As shown in Figure 1.15, with Hinode observations, we can know the magnetic energy stored in corona before magnetic reconnection (top part of Figure 1.15). The most part of energies can be evaluated in the post reconnection stage after the transient energy release is finished (bottom part of Figure 1.15). On the other hand, there is poor observational knowledge on the physical parameters in the reconnection region during the period when the reconnection process is on going (middle part of Figure 1.15). The inflow into the reconnection region, the plasma temperature in the reconnection region, and the temperatures and densities of the plasma jets (outflows) have not been measured quantitatively. They are key observational parameters necessary for probing reconnection process.

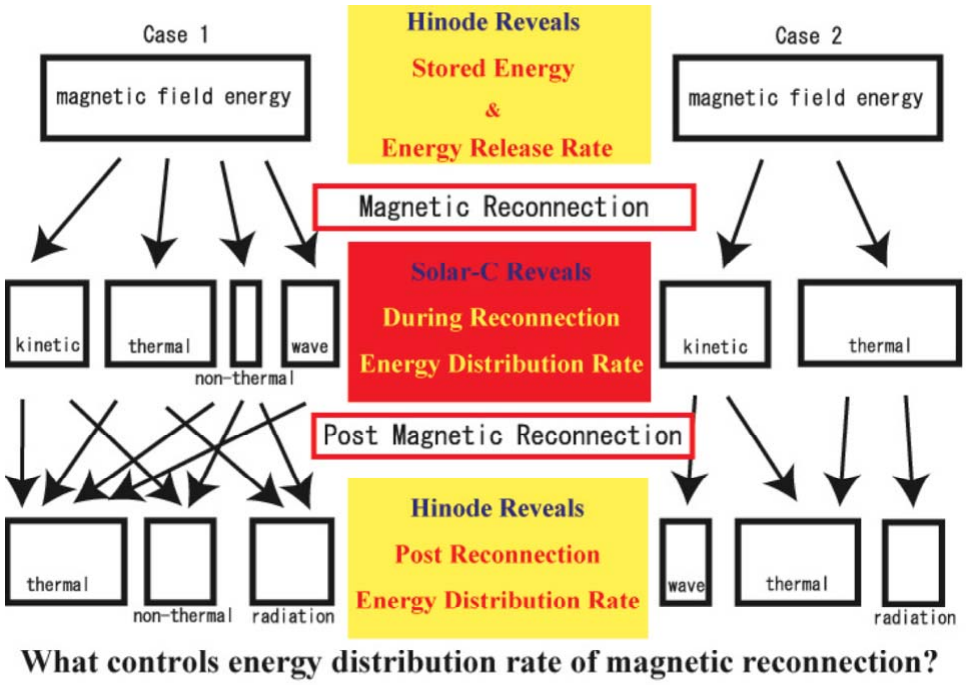

Figure 1.15. Energy distributions during magnetic reconnection.

1.3.4.2. Probing inside the reconnection region in non-ionization equilibrium

Theoretical model of steady fast reconnection, called Petchek-type reconnection, expected the formation of two slow-mode shocks elongated from the reconnection region, which play a role in heating ambient plasma. During rapid heating with slow-mode shocks, heated plasma would be in non-thermal equilibrium condition. There are typically three kind of thermal non-equilibrium conditions; 1) Non Maxwellian energy distribution, 2) different temperature in different species (e.g., Tp > Te), and 3) transient ionization condition (ionization

non-equilibrium). All of three conditions are predicted in the reconnection region, and the detection of them are a challenging target for Solar-C.

Figure 1.16 shows a calculation of non-equilibrium ionization structure in 1200 km/s jets at the down stream of magnetic reconnection region. We can clearly see that the plasma state in the downstream of slow shocks cannot reach to ionization equilibrium. The proposed high-throughput EUV spectrometer (~10 times better than the effective area of the currently available spectrometer, see Figure 3.3 in Chapter 3) can measure spectral lines with much shorter exposures, allowing detecting the transient state of non-ionization equilibrium. Such transient state tells us a history of ionization process of each ion and thus contains the information of the reconnection region. For detecting the transient ionization condition, a lot of spectral lines covering a broad range of ionization states need to be measured, which can be done only with the proposed UV/EUV spectrometer (for flare plasma, from Fe XVIII to Fe XXIV, see Appendix 3-A).

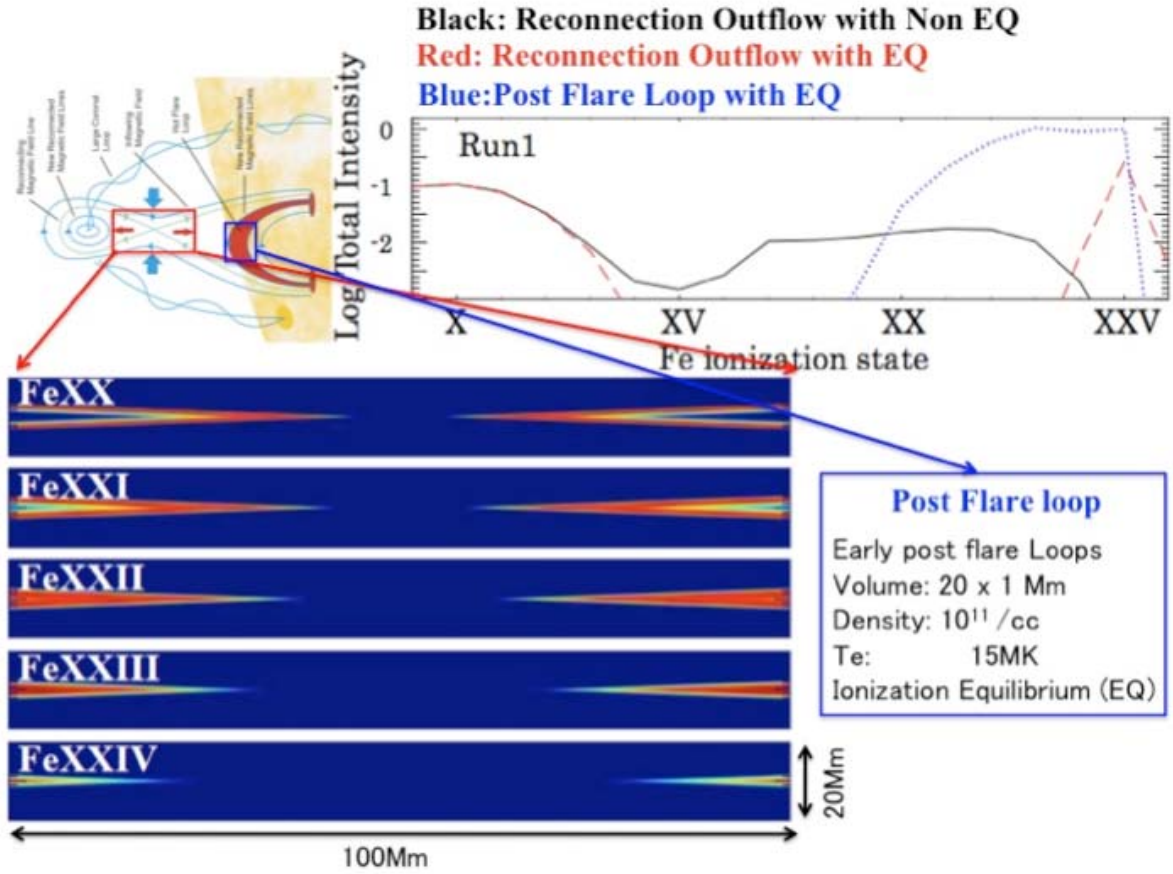

Figure 1.16. A computation of non-equilibrium ionization structure in 1200 km/s jets at the down steam of magnetic reconnection region. The following parameters are used in this computation: magnetic field 12 gauss, electron density 4.2×10^8cm-3, temperature 1MK, and plasma β 0.01 at the upstream side of the slow-mode shock and temperature 40MK at the downstream; the shock angle at the upstream and downstream is 85 deg and 2.3 deg, respectively. The upper right panel shows the total intensity of the non-equilibrium ionization structure (black line) as a function of ionization state is compared with the total intensity of post-flare loop (blue dotted line).

The signal intensity of the non-equilibrium ionization structure can be seen in contrast with the bright post-flare loop, if we choose suitable spectral lines (Fe XV ~ Fe XVIII). Bright flare

loops have typical temperature of ~10 MK and density of ~10^{11}cm^{-3}, and therefore the loops are dominantly observed with Fe XIX ~ Fe XXII. In the reconnection region, it takes ~100s to reach the ion state to higher ionization states after the energy release in a short time scale. Thus, we expect that signals exist not only in high ionization states (Fe XVIII ~ Fe XXIV) but also in low ionization states (Fe XII ~ Fe XVII).

When spectral lines with ionization states higher than Fe XIX are used for measurements, observing the early phase of solar flares is a key to success the diagnostics of the reconnection region. This is simply because bright flare loops developed during flares has higher density, say, by two orders of magnitude, than the density inside the reconnection region. This means that the spectral line intensities from the flare loops are higher by four orders of magnitude than that of the reconnection region. In the early phase, the total emission measure of flare loops is still small and thus we have possibility to detect signals from the reconnection region, when we have the spectrometer with wide dynamic range and low scattered-light optics.

In the down stream of slow-mode shocks, the ion temperature may not be same as the electron temperature. Such non-equilibrium is frequently observed in collisionless plasma condition (Baumjohann et al., 1999). To understand how much energy is given to ions and electrons respectively, we should observe both of ion and electron temperatures simultaneously. Line width of EUV spectral lines can be used to estimate ion temperature (e.g., Imada et al., 2009), but the ionization equilibrium is always assumed in the spectroscopic analysis of EUV lines, resulting in difficulty in deriving electron temperatures for transient non-equilibrium plasma. Therefore it is essential to have another measurement for deriving the electron temperature inside the magnetic reconnection region. Accurate measurements of the electron temperature can be achieved by measuring thermal bremsstrahlung emission at short wavelengths (soft X-rays) with the proposed photon-counting X-ray telescope. In contrast to the EUV line spectroscopy, the spectral shape of thermal bremsstrahlung emission directly reflects the electron temperature without depending on the ionization equilibrium.

Because of its faint structure, non-ionization equilibrium signals inside the magnetic reconnection region are not easy to detect. But the proposed UV/EUV high-throughput spectroscopic telescope has potential to detect them, because of its high-throughput performance and low scattered optics. If we can observe inside the reconnection region, then we can determine the reconnection condition by using the knowledge of non-ionization equilibrium. The ionization process is similar to the nuclear-decay process. Thus we can estimate the time passage from strong heating. The velocity, density, and ion temperature in the reconnection region can be derived from line spectroscopic analysis with the knowledge of non-ionization equilibrium plasma. Therefore, probing the magnetic reconnection region from viewpoint of non-ionization equilibrium can provide useful information on the mechanisms of the energy distribution rate.

1.3.5. Particle Acceleration coupled with Reconnection Dynamics

Yohkoh observations played an important role in revealing particle acceleration mechanism in solar flares. A loop-top hard X-ray source was discovered in a compact flare (Masuda et al. 1994), indicating that energy release and particle acceleration occurs above the post-flare loop. Using a unique technique “time-of-flight method,” Aschwanden et al. (1997) also showed that the particle acceleration occurs above the post-flare loop. It is currently believed that particles are accelerated in the current sheet and slow/fast-mode shocks coupled with the reconnection dynamics. However, we have not at all understood how particles (ions and electrons) are

accelerated. This is because of the difficulty in directly probing the acceleration region. One of the main reasons for the difficulty is the lack of dynamical range in hard X-ray observations.

Accelerated electrons radiate X-ray emissions via non-thermal bremsstrahlung process. The amplitude and energy of X-ray emissions depends on the number and energy of accelerated electrons. An impediment to fully understanding of acceleration mechanism is a dynamic range of instrumentation. The proposed photon-counting grazing-incidence X-ray telescope has dynamic range three orders of magnitude better than RHESSI. It covers the energy range from <1 to ~5 keV (goal ~10 keV), which contains thermal emission both in continuum and lines as well as non-thermal emission at the higher end of the energy range. Suprathermal electrons (~10keV) have most parts of non-thermal energy. Non-thermal signatures have been seen even below ~5 keV in many microflares (Hannah et al. 2008). Therefore, the proposed X-ray telescope may allow us to evaluate non-thermal electrons.

Another way to discuss the non-thermal energy is by determining whether the electron energy distributions are Maxwellian or not with the EUV spectroscopic measurements. Seely et al. (1987) studied the change of line intensity ratios of He- and Li-like Fe ions with non-Maxwellian electron energy distribution in the laboratory experiment. The bottom two panels of Figure 1.17 show Fe XIV lines with thermal and non-thermal equilibrium conditions. They show that intensity ratios marked with red circles changes in these two cases. Differential emission measure and electron density can affect on the intensity ratios, as well as non-thermal equilibrium state. Therefore, multiple line observations (see Appendix 3-A) can distinguish which affect on the intensity ratio. The Hinode EIS cannot perform such analysis because of poor wavelength coverage, but the proposed UV/EUV spectrometer will provide a quantum leap in our understanding of electron energy distributions and particle acceleration in the solar atmosphere.

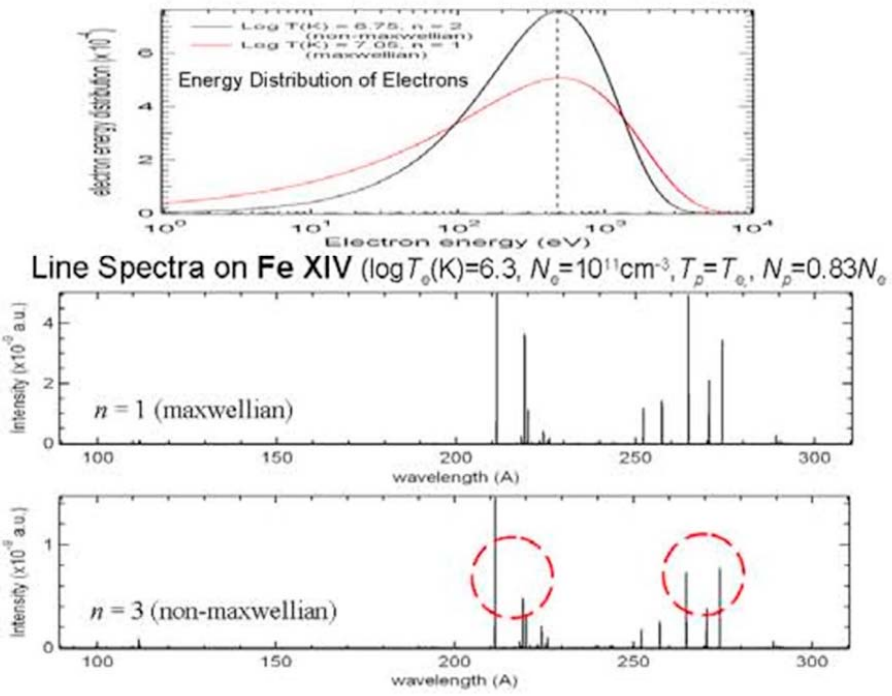

Figure 1.17. Two electron energy distributions corresponding to Te ~ 650 eV (top panel) and changes of Fe XIV line intensity ratios (bottom panel) highlighted by dotted red circles.

1.3.6. What is the role of 3-dimensionality in magnetic reconnection?

Another important question in solar flares is what is the role of 3-dimensionality in magnetic reconnection. Generally the current sheet thickness of the magnetic reconnection is in order of ion inertia/gyro radii scale (a few 10m). However, solar flares show a large (a few 100Mm) well-known flare arcade and ribbons (see Figure 1.19). The difference of scale size between current sheet thickness and current direction is roughly 7 orders of magnitude. The question is that the magnetic reconnections take place individually in current direction, or there are some causal connections for current direction. In other words, we can say that the simultaneous flare triggers happen in each current sheet and they are developed to a large flare structure, or only one local flare trigger happens and the former magnetic reconnection causes the latter magnetic reconnections. To clarify this point, we should investigate that the existence or nonexistence of the causal connection for current direction in solar flares.

One of the advantages on using the solar plasma for magnetic reconnection studies is that imaging observations of reconnection events, such as flares and jets, can provide the global picture of plasma condition and magnetic field configuration. We already have some indication from modern satellite observation, and many modeling study has been done. According to their result, flare arcades must be individually heated as large numbers of distinct loop strands in order for them to reproduce the observed emission signatures (e.g., Hori et al. 1997; Reeves & Warren 2002; Reeves, Warren, & Forbes 2007; Warren & Doschek 2005). This multi-loop model provides a good description of a coronal arcade once it has come to rest after a flare reconnection event. Some theoretical studies show that patchy reconnection (Figure 1.18) can create a large number of distinct reconnected loops which each descend individually through the corona. Although we know that each post-flare loops have different characteristics, we do not have enough information about the causal connection for each flare loops. To clarify this point, we need spectroscopic observation (Doppler shifts and line width) with high temporal resolution. If there are some relationships between each flaring loops, the information of triggers may propagate with Alfven speed. Thus at least we need temporal resolution shorter than Alfven transit time. Therefore, spectroscopic measurements with high cadence (shorter than Alfven time) can open a new window for investigating the role of 3-dimensionality in magnetic reconnection.

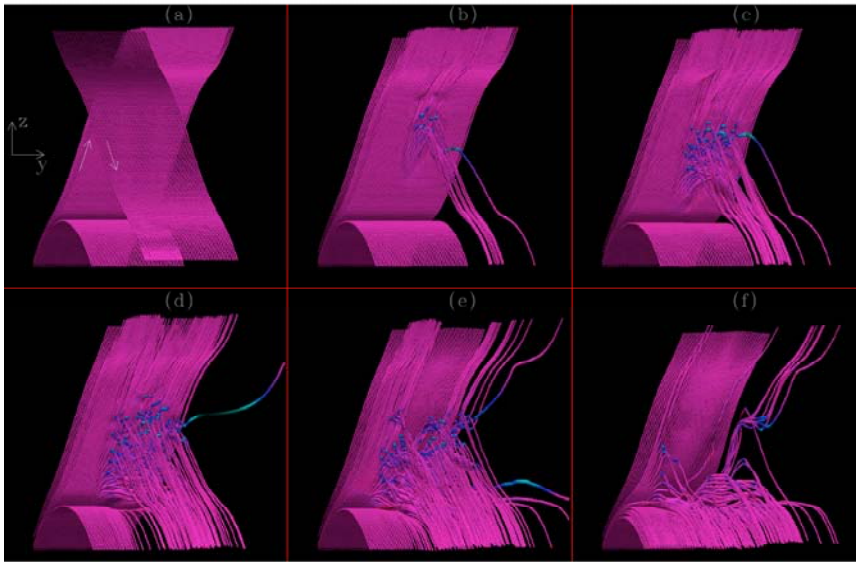

Figure 1.18. Field connectivity change predicted in patchy reconnection

1.4. Small-scale Physics Initiating Large-Scale Phenomena

1.4.1. Flares and CMEs

Solar flares and coronal mass ejections (CMEs) are manifestations of explosive energetic events at the Sun that accelerate particles. Both sources cause geo-effective particle events that endanger space assets and human explorers.

1.4.1.1. Coronal Magnetic Fields for Initiating CMEs and Flares

The start of most CMEs is associated with the eruption of a prominence/filament or sigmoid. Both prominence/filaments and sigmoids are manifestations of non-zero magnetic helicity; that is, they show evidence of non-potential magnetic fields, and thus electric currents and twisted magnetic fields. Both have been modeled as magnetic flux ropes (e.g., Rust & Kumar 1996; Titov & Demoulin 1999). Essentially all models of sigmoid formation involve twisted ropes of magnetic flux, since the twist affords a convenient method of storing energy needed for an eruption, and the appearance of the sigmoids is suggestive of writhing coronal loops (McKenzie & Canfield 2008; Savcheva & van Ballegooijen 2009).

The presence of measurably twisted fields before the eruption facilitates an estimation of the stored energy available for the eruption. The coronal magnetic fields are modeled primarily with a non-linear force free field (NLFFF) model. The magnetic fields measured at the photospheric level are currently used for this modeling, but the photospheric data are not consistent with the NLFF condition. The force-free condition is well justified in low beta plasma, which is in the corona and the upper chromosphere and is not in the photosphere. Nevertheless, precise photospheric vector magnetic field data from Hinode is currently the most key observation for NLFFF modeling of coronal fields in data-driven simulation of large flares and CMEs (e.g., Kataoka et al. 2009). The data-driven simulation will be a powerful method for understanding what triggers eruptions, flares, and CMEs. It is desirable to establish a reliable method for measuring the Poynting flux in an active region in order to calculate the available free energy for an eruption. Predicting the size of an eruption is important for space weather applications.

Magnetic fields measured in the chromosphere will be a key for improving the accuracy of NLFFF modeling. Direct chromospheric magnetic field information, e.g. Hα images can be used as additional constraint (Wiegelmann et al. 2008). Hα images show the horizontal direction of the chromospheric magnetic field vector. Direct measurements of line-of-sight chromospheric magnetic field help to serve as an additional constraint. Measurements of the magnetic field vector in the low beta chromosphere could be used directly as boundary condition for NLFFF modeling.

An important issue for NLFFF-modeling is to have sufficient large field of view that accommodates most of the connectivity within a region and its surroundings (DeRosa et al. 2009). Because of narrow field of view (200 arcsec x 200 arcsec), the high spatial resolution magnetic field data from Solar-C needs to be imbedded into a large field of view data from other spacecrafts, such as Solar Dynamic Observatory (SDO), and ground-based observatories. Therefore, for accurately estimating the magnetic field of flares and CMEs in the corona, it is most important to coordinate the Solar-C observations with instruments with wide field of view, such as SDO and ground-based observations.

1.4.1.2. Small Scale Triggers and Dynamics in Initiation

In order to accurately predict when, where, and how space weather events are initiated, we must understand the interrelationship between small-scale processes on the solar surface and large-scale magnetic structures in the solar corona. In particular, current belief is that small-scale processes (e.g., magnetic reconnection) are important as a trigger for solar flares. The solar magnetic fields control the flow of energy and formation of structures above the photosphere. Hinode observations would make much more progress in understanding the role of magnetic topology (such as quadrupolar fields in the breakout model) and small-scale photospheric flux emergence in flare and CME initiation, if Hinode captures many more flare events in coming years. Flux emergence is one of key magnetic activities in the photosphere to quickly develop magnetic topology for flare and CME initiation.

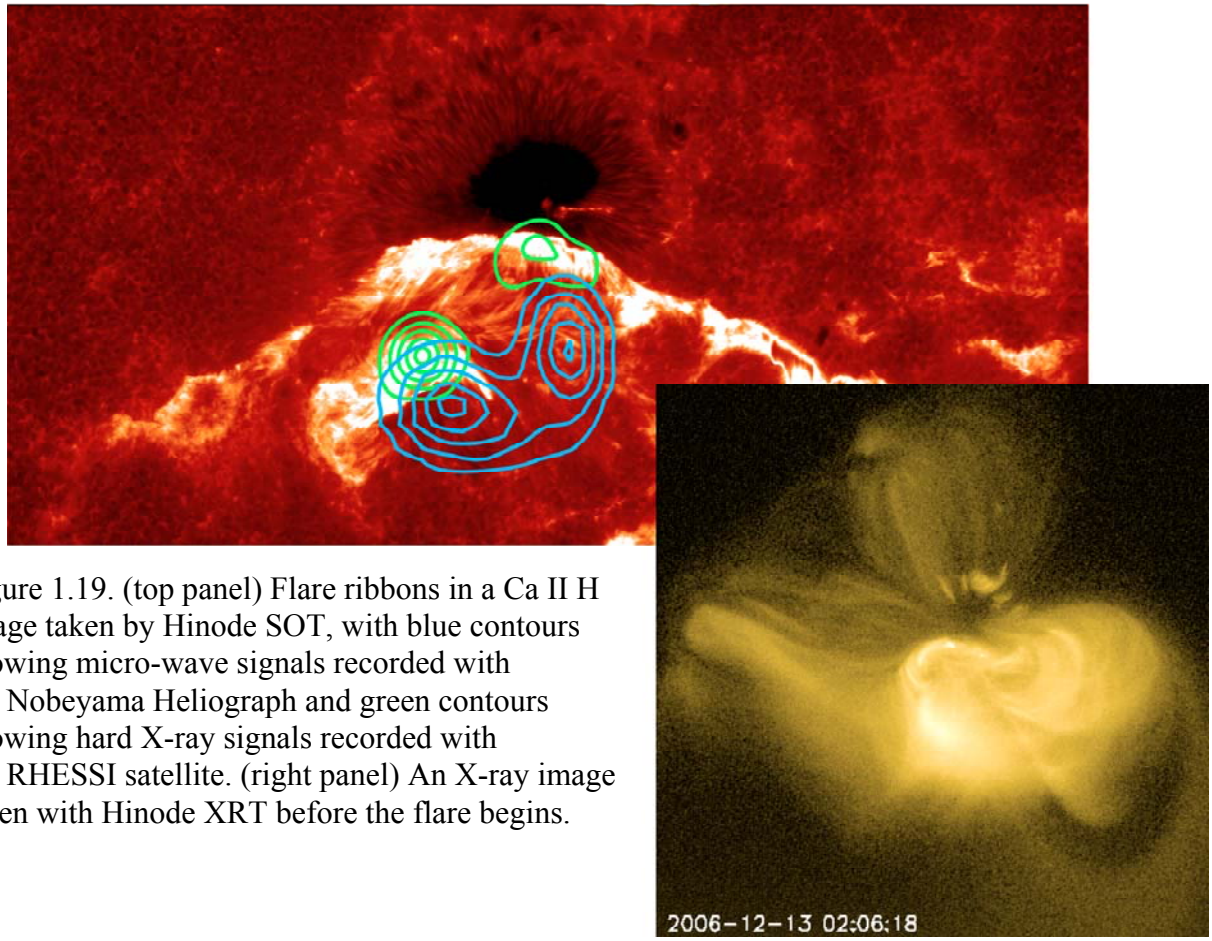

Figure 1.19. (top panel) Flare ribbons in a Ca II H image taken by Hinode SOT, with blue contours showing micro-wave signals recorded with the Nobeyama Heliograph and green contours showing hard X-ray signals recorded with the RHESSI satellite. (right panel) An X-ray image taken with Hinode XRT before the flare begins.

Measurements of magnetic fields in the higher layer, i.e., chromosphere, and mass flows over the entire atmosphere will observationally provide new insights in understanding flare and CME initiation. For example, many flares are related to newly emerging flux, and the higher the complexity and shear of the field the greater the chance of flares occurring. We do know that there is a 'time lag' from when flux emerges to when there is a response in the corona (e.g. Schmieder et al., 2004). Flux emergence can occur 6 hrs before a flare occurs. In the 13th December 2006 X-flare (Figure 1.19), the increase in coronal turbulence occurred 12 hours before the flare began (Harra et al., 2009) and 16 hours after the helicity injection rate reached a peak (Magara and Tsuneta 2008). Further work studying the detailed response of the

chromosphere and corona to emerging flux has shown that the chromospheric response occurs first (Li et al., 2007). There is also evidence that the corona shows a small increase in flows before flaring begins (Harra et al., 2010). The chromospheric emission shows small brightenings over the complex region of emerging flux. The corona behaves in a completely different way, showing the development of large-scale loops with enhanced outflows at the edges. The linkage between the chromosphere and corona nor the energy transport processes that follow the flux emergence are not understood yet. Theoretical simulations have been carried out to explain flux emergence (e.g. Cheung et al., 2008), but the full connection from below the photosphere to the corona and the linkage with magnetic reconnections in corona and chromosphere is not yet achievable.

Flare initiation studies will be partially performed with Hinode, if Hinode captures many more flare events in coming years. With this in mind, we define the Plan B science goals more specifically. Hinode can provide accurate measurements of vector magnetic fields at the photospheric level, but such maps covering a large area are available only with extremely long interval (several hours or longer). Considering the timescale of emergence of each magnetic flux (5-15 minutes to cross from the photosphere to the corona), much increase of cadence will allow us to capture details of the flux evolution. Enhanced telemetry resource about one order of magnitude larger than Hinode will increase mapping cadence to less than several tens of minutes even for a large field of view (200”x200”) with 0.2” resolution. In addition, measurements of chromospheric magnetic fields can provide the dynamical evolution of emerging flux and nearby pre-existing flux in 3D domain.

There are some signatures of changes in the corona before a CME erupts, e.g., increasing coronal flows (Baker at al., 2009). This indicates that the overlying magnetic fields are changing which reduces the stabilizing forces of the overlying magnetic field. The energy necessary to produce these changes clearly comes from magnetic fields that emerge from below the surface, but the mechanism for transporting this energy to regions above the surface is unclear, including its effect on the moment the CME is triggered. Current indications are that reconnection must be occurring in the lower atmosphere to build up the pre-eruption magnetic structure of a flux rope (Green and Kliem, 2009). But this cannot be presently modeled due to lack of spectral information in the low atmosphere. EUV/FUV spectroscopy covering from the low atmosphere to the corona can reveal the entire picture of mass flows.

1.4.1.3. Fine Magnetic Field Structures in Prominences/Filaments

A typical prominence – filament on the disk – is characterized by chromospheric cooler material (about 10,000 K) suspended at coronal heights, a configuration that can only persist if the magnetic field supports the plasma against the force of gravity. Since major flares and CMEs are sometimes accompanied by an eruption of the prominence, the formation and dynamics of the prominence is also essential to address questions of magnetic energy storage/release for a CME-like explosion.

Hinode SOT observations have revealed that prominences have very complicated geometrical configurations, and they look different in active region and quiet Sun (Figure 1.20); Active-region prominence consists of nearly horizontal threads (Okamoto et al. 2007, Merenda et al. 2007), whereas quiescent prominence has apparent vertical threads (Berger et al. 2008), although magnetic field is supposed to be oriented horizontally. Prominences are also supposed to have helical magnetic configuration to support cool materials in the corona, but there is no direct magnetic field measurements to confirm the helical configuration in prominence.

Direct measurements of magnetic fields in prominences have been required to reveal the overall magnetic field configuration in prominence and how the configuration is developed. Weak magnetic fields in prominences produce polarization signals by so-called Hanle effect and therefore magnetic field orientation can be inferred with sub-arcsec spatial resolution when the polarization profiles of chromospheric lines are measured with the proposed 1.5m telescope (SUVIT). It would be a great progress in understanding the triggers of CMEs and flares, if the magnetic fields can be measured during the eruption of prominences.

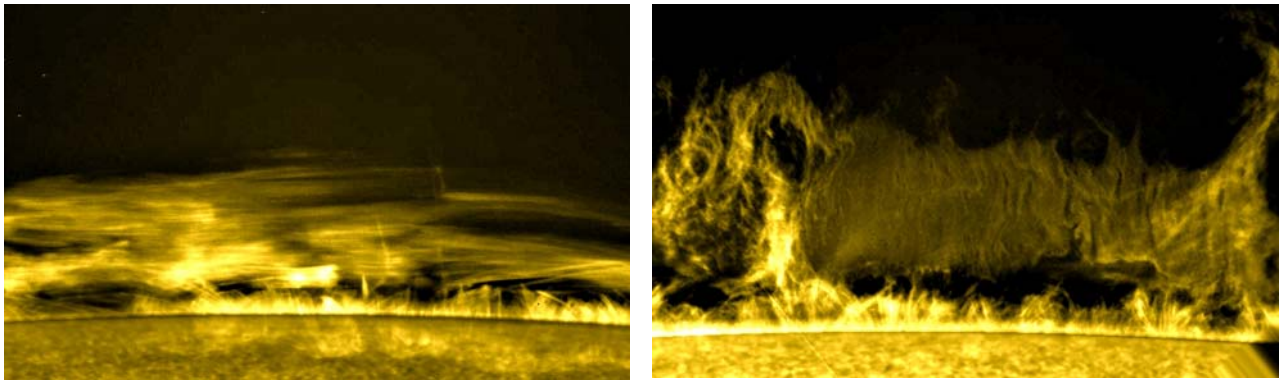

Figure 1.20. Prominences observed in an active region (left) and a quiet region (right) with Hinode. It is important to clarify how the fine structures smaller than 1 arcsec are associated with magnetic field configuration.

1.4.1.4. Solar Flare Forecasting

One of the most important goals of solar physics research is to improve our ability to predict geo-effective solar flares and CMEs. The Solar-C mission has observational capabilities to advance our understanding and prediction capability for space weather, primarily by exploring how small-scale physical processes are related to the initiation of space-weather phenomena.

It is empirically known that the occurrence rate of big solar flares correlates with some extensive quantities representing the properties of magnetic field and flow in flaring active regions. For instance, the probability for big flares to occur within 24 hours exceeds 50% in big active regions, where the extensive magnetic quantity, e.g. unsigned magnetic flux, is larger than some critical value. However, the skill score for forecasting flares is still low, and it is too difficult to predict the onset of solar flares with high reliability (Leka and Barnes 2007, Barnes and Leka 2008). It is due to the fact that the major fraction of flares occurred in moderate active regions, where the extensive quantity is lower than the critical value. The result indicates that the extensive quantities, which can be obtained by the integration over whole active region, cannot provide us sufficient information to forecast solar flares, and also suggests that the occurrence as well as the scale of solar flares is susceptible to the trigger process, which might proceed in much smaller region than the size of active region. Therefore, to identify the critical indications of flux emergence that causes flares and CMEs is crucial for developing flare prediction algorithms. If we can discriminate the small-scale activity triggering solar flares in terms of the unprecedentedly high resolution observation, it would be likely that the predictability of solar flares could be improved and that the Solar-C would greatly contribute the space weather forecast.

1.4.2. Solar Winds

1.4.2.1. Origins of Fast Solar Winds

Coronal holes (CH) are the source of the fast solar wind (Krieger et al. 1973). For polar coronal holes, Hassler et al. (1999) found regions of strong outflow lying at the boundary of magnetic network cells from observations in the λ770A Ne VIII resonance line formed at the base of the corona (T=0.63 MK). Outflows are also seen in the much cooler λ584A (Wilhelm et al., 2000) and λ10830A (Dupree et al., 1996) He I lines. Tu et al. (2005) find that the wind starts flowing between 5 Mm and 20 Mm from the measurement of C IV and Ne VIII, respectively. However, there is still a substantial lack of knowledge on which structures within coronal holes, and what physical mechanisms, are primarily responsible for the wind acceleration. Three candidates have been discussed as the structures responsible for the fast solar wind: plumes, interplumes, and jets (Figure 1.21).

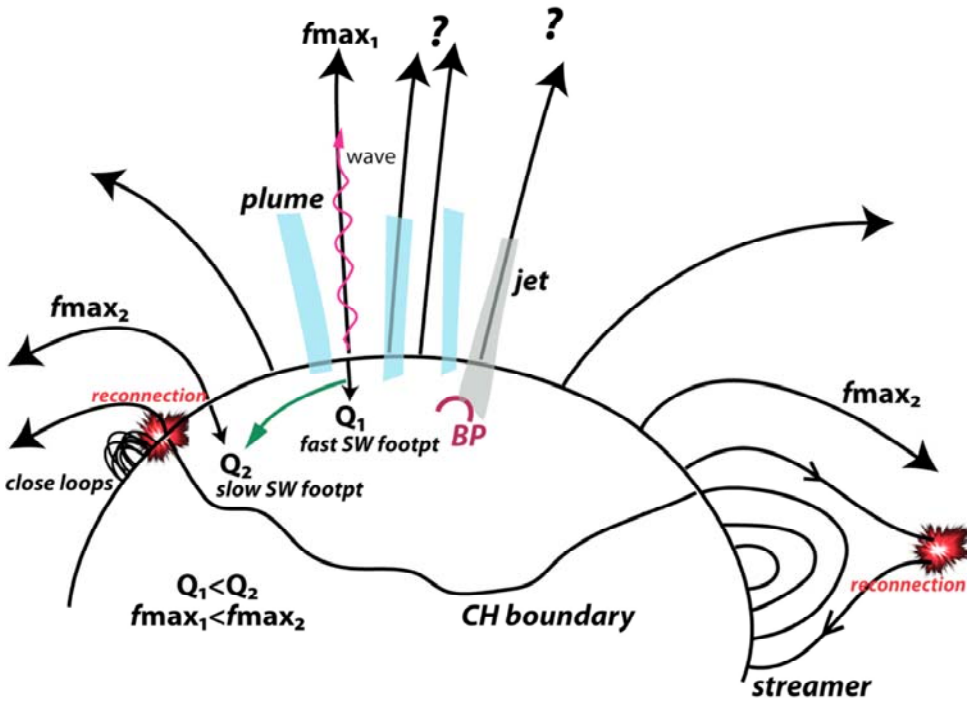

Figure 1.21. Some possible sources of the fast solar wind (plume, interplume, jet) and slow solar wind (coronal hole-steamer boundary, edge of active regions, reconnection between open field lines and close loops, reconnection at streamer stalk).

Being the most prominent feature within CHs, plumes have been and are considered as a strong candidate for the source regions of the fast wind, but theoretical models give opposite indications; Del Zanna et al. (1997) and Casalbuoni et al. (1999) show that the outflow speed in plumes can be larger or smaller than in the ambient depending on the temperature and Alfvén wave flux assumed in the two regions. VUV lines formed around 1 MK allow the study of the plumes roots on the disk where their intensity is enhanced with respect to the background CH emission. In addition to measuring Doppler shift along line of sight, Doppler dimming features seen in, for example, O VI 103.2/O VI 1037A lines allows to determine the radial component of

the plasma outflow velocity from the analysis of off-limb spectra, although some assumption on the geometry of coronal structures is necessary. From SUMER and UVCS combined data, Teriaca et al. (2003) derived the outflow vs. altitude profile in interplumes. However, the result for the plumes is controversial with very different results being present in the literature (Giordano et al. 2000; Gabriel et al. 2003, 2005; Raouafi et al. 2007). Jets are often associated to plums (Raouafi et al. 2008), which may cause different results, because the integration of signals recorded by the 36 to 48 hours' SUMER observations is required to derive reliable results. High throughput performance improved by one order of magnitude from SUMER will allow us to study time variability of outflows at timescale of a few hours. From EUV spectroscopy, plumes are known to be denser and cooler than the surrounding interplume regions (e.g., Wilhelm 2006). Spectral lines are observed to be broader in interplumes (e.g., Wilhelm, 2006; Banerjee et al. 2000) hinting at preferential energy deposition in these structures. Signatures of slow magnetoacoustic waves have also been found in both plumes (DeForest & Gurman 1998, Ofman et al. 1997; 2000) and interplume regions (Banerjee et al. 2000; 2009), and it is important to understand observational link between waves and velocity structures (see also section 1.2). Moreover, the spectroscopic analysis of chemical composition could provide a tool to establish whether plumes or interplume regions contribute significantly to the fast wind by comparing the composition of the different structures on the Sun with in situ data.

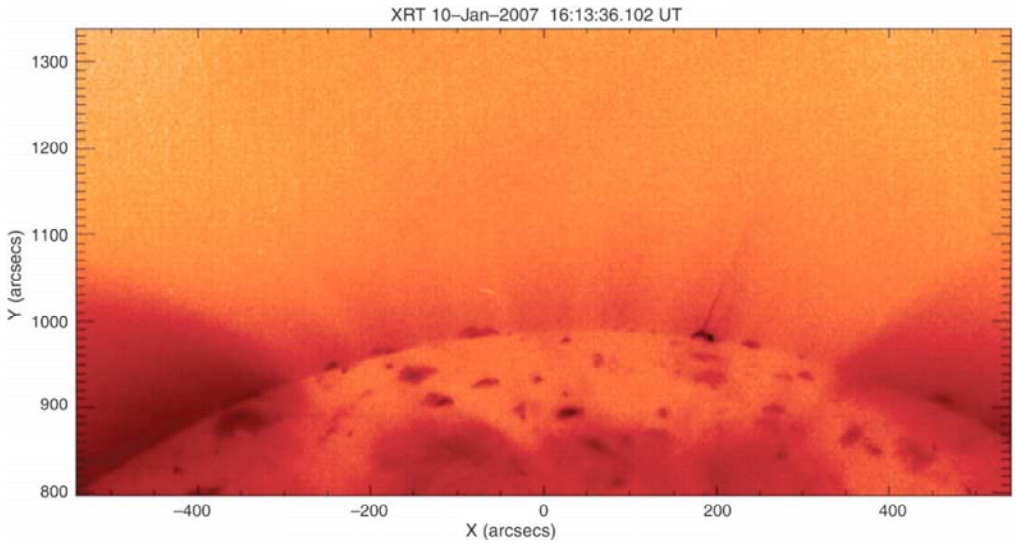

Figure 1.22. Hinode XRT false-color image of the north polar coronal hole. A typical jet is seen in the center of this image (from Cirtain et al. 2007).

The Hinode XRT has revealed a large number of jets occurring within the polar holes (Cirtain et al., 2007, Figure 1.22). Given the high velocities attained during these events (up to 800 km/s), they may be contributors to the wind. The Hinode SOT has revealed wide distribution of strong field patches in the polar regions (Tsuneta et al. 2008, Figure 1.23), by viewing the polar regions at 7 deg inclination periods with 0.3 arcsec spatial resolution. Flux emergence appears into open fields (e.g., coronal holes), resulting in jets (e.g., Shimojo and Tsuneta 2009). The standard model for jets associates the energy source with reconnection in the corona, but detailed chromospheric and transition region diagnostics are currently not available. Current observations also lack the spatial resolution to see the sub-structure of jets. Jets are important targets for close examination because they are the most likely place to observe reconnection and its related sub-structure in the corona. Because of the relatively small scale of jets, a reasonably accurate accounting of the magnetic flux budget, and the energy budget, should be

achievable with high-resolution, high-sensitivity photospheric and chromospheric magnetograms, paired with high-resolution, high-sensitivity, high-cadence coronal imagery. Such studies should enable measurements of the energy storage prior to jet eruption, the rate of energy release, and the rates of helicity transfer. In light of the Hinode observations of coronal jets, it is believed that the jets may contribute a significant amount of mass into the fast solar wind.

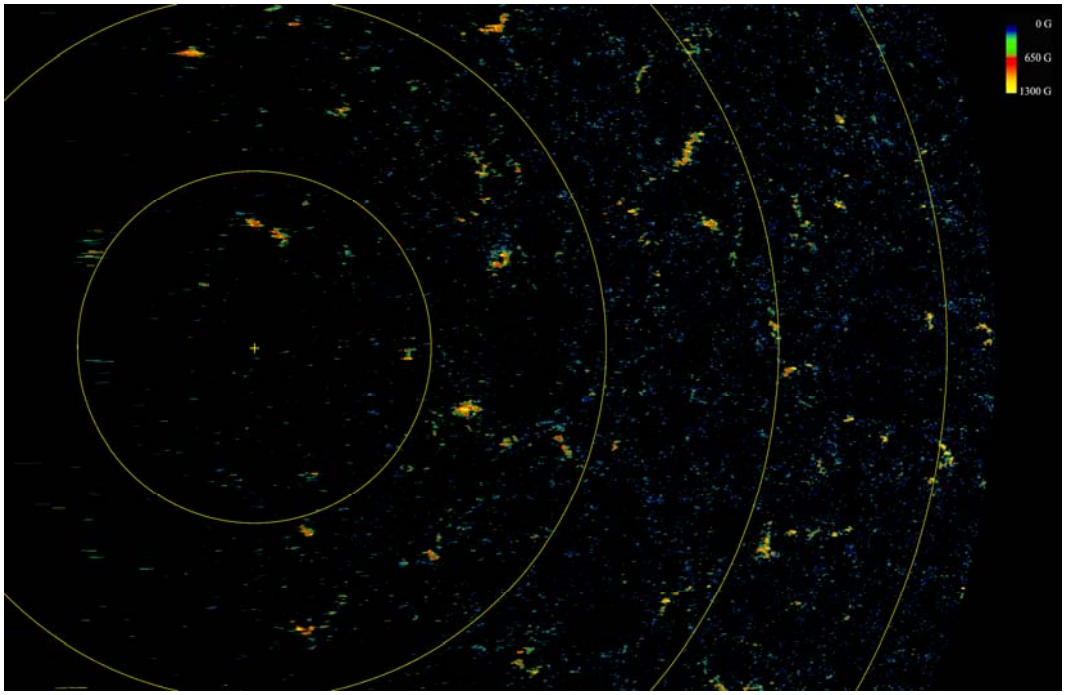

Figure 1.23. Strong patches of kG magnetic fields distribution in the polar region, reveraled with Hinode SOT magnetic field measurements (Tsuneta et al. 2008).

1.4.2.2. Origins of Slow Solar Winds

The source of the slow solar wind is even more difficult to identify than that of the fast solar wind. Sources include coronal holes boundaries, edges of the streamer belt and edges of active regions (Figure 1.21). The proposed UV/EUV spectrometer is capable of measuring relative element abundances in different atmospheric structures that can be related to in-situ measurements from Solar Orbiter and Solar Probe+. The abundances in the slow solar wind are different from in the fast solar wind. Thus, abundance measurements can be used with in-situ measurements to locate the origins of the slow solar wind. The Hinode observations have revealed the persistent flows at the edges of active regions (Figures 1.24, Sakao et al. 2007). These could provide up to 25% of the slow solar wind. Recent STEREO and Wind observations suggest that a considerable fraction of the slow solar wind is transient in nature even at solar minimum – these have small scale-sizes and low magnetic field strength. They seem to be related to coronal source surface sector boundaries (Kilpua et al., 2009) that could be dynamical changes at coronal hole boundaries or edges of helmet streamer belts. The process involved is not fully understood and it is widely debated whether these outflows are caused by waves or reconnection. Certainly the magnetic configurations involved suggest large-scale magnetic reconnection, however there is also some evidence for wave-like behavior of the outflow. The in-situ composition data for these transient slow winds seem consistent with open-field regions,

rather than closed-field regions. The proposed UV/EUV spectrometer can measure abundances throughout the atmosphere and map the differences and determine how the abundances evolve.

The active region upflow speeds derived from spectral line wavelengths vary with spectral lines formed at different temperatures, which implies that the upflows consist of fine scale structures with difference speeds. At present it is impossible to connect these flows with transition region and chromospheric structures, due to the limited wavebands and spatial resolution of Hinode EIS. If we are going to understand how these flows arise, i.e., the source of their energy, and where in the atmosphere they originate, a higher spatial resolution instrument with connectivity to lower temperatures is essential.

To make further progress, it is necessary to sort out properties of the solar wind source regions among a variety of possible source structures. It is important to 'follow' the field lines from the chromosphere, through the transition region, up into the corona by comparing and relating plasma properties such as density, temperature, line width, Doppler shift and elemental abundance, in space and time across the footpoint region of slow wind. At the same time, magnetic field extrapolations are needed to identify preferable location of magnetic reconnections in the transition region and corona and to show the connections to the heliosphere.

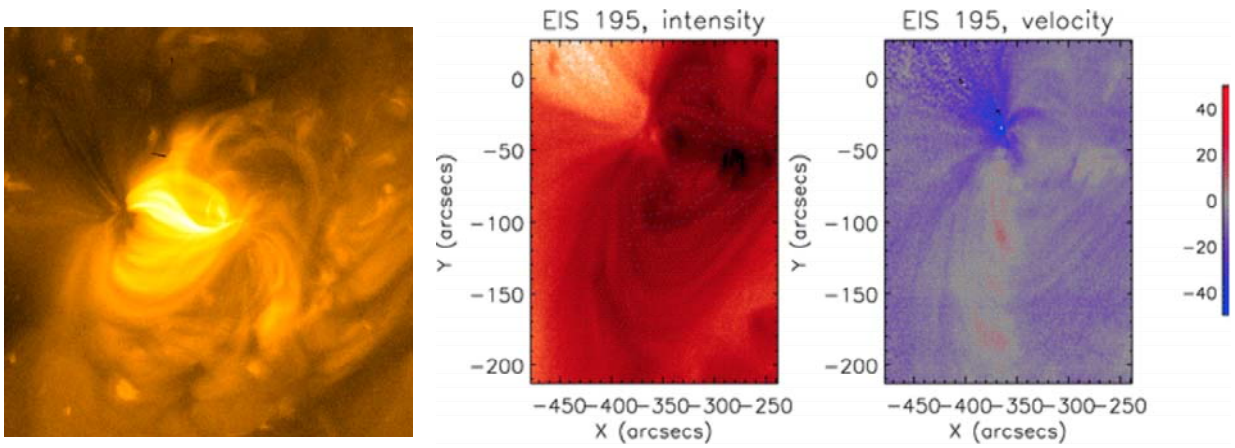

Figure 1.24. Persistent plasma outflows at the edges of action regions, revealed with Hinode observations.